

# Selecting ChIP-Seq Normalization Methods from the Perspective of their Technical Conditions

Sara Colando, Danae Schulz, and Johanna Hardin

January 7, 2025

## Abstract

Chromatin immunoprecipitation, followed by high throughput sequencing (ChIP-Seq) provides vital insights into locations on the genome with differential DNA occupancy between experimental states. However, since ChIP-Seq data is collected experimentally, it must be normalized between samples in order to properly assess which genomic regions have differential DNA occupancy via differential binding analysis. While between-sample normalization is a crucial for downstream differential binding analysis, the technical conditions underlying between-sample ChIP-Seq normalization methods have yet to be specifically examined. In this article, we identify three important technical conditions underlying ChIP-Seq between-sample normalization methods: symmetric differential DNA occupancy, equal total DNA occupancy, and equal background binding across experimental states. We categorize popular ChIP-Seq normalization methods based on their technical conditions and simulate ChIP-Seq read count data to exemplify the importance of satisfying a normalization method’s technical conditions to downstream differential binding analysis. We then assess the similarity between normalization methods in experimental CUT&RUN data to externally verify our simulation findings. Both our simulation and experimental results underscore that satisfying the technical conditions underlying the selected between-sample normalization methods is crucial to conducting biologically meaningful downstream differential binding analysis. As such, we suggest that researchers use their understanding of the ChIP-Seq experiment at hand to guide their choice of between-sample normalization method when possible. Alternatively, researchers could use the intersection of the differentially bound peaksets derived from different normalization methods to determine which regions have differential DNA occupancy between experimental states when there is uncertainty about which technical conditions are met.

## 1 Introduction

In the recent decades, high-throughput sequencing has become one of the most popular methods for data generation in genomics, epigenomics, and transcriptomics [14]. A popular method of high-throughput sequencing is chromatin immunoprecipitation followed by high-throughput sequencing, or ChIP-Seq. ChIP-Seq typically involves shearing the DNA via sonication before conducting immunoprecipitation with an antibody that is known a priori to bind with the protein of interest (i.e., transcription factor, histone modification, etc.). Ideally, only the DNA fragments which are occupied by the protein of interest will remain after immunoprecipitation. These remaining fragments are then purified and sequenced before being aligned to a reference genome [20]. The aligned *reads* (i.e., sequenced DNA fragments) are then used to characterize the amount of occupancy of the protein of interest within a specific genomic region [26].

Given that ChIP-Seq experiments are conducted to assess which genomic regions are truly occupied by the protein of interest or, further, whether there is a change in the amount of protein occupancy in specific genomic regions across different experimental states, *peaks* (i.e., genomic regions enriched with DNA binding) typically serve as the unit of interest in ChIP-Seq data analysis. In this article, we refer to *DNA occupancy (per cell)* as the population parameter that we aim to estimate using ChIP-Seq data analysis and the sample estimate of the DNA occupancy (per cell) as the *DNA binding (per cell)*. In this sense, a peak is considered *differentially bound* if there is a statistically significant difference in the amount of DNA binding in the

peak region between the experimental states [19].<sup>1</sup> The raw amount of DNA binding within a given peak is calculated by counting up the number of reads aligned to the specific genomic region. Generally speaking, genomic regions with higher read counts, i.e., more DNA binding (per cell), are expected to have a higher amount of DNA occupancy (per cell), on average [19].

However, since ChIP-Seq data is collected experimentally, there are expected to be differences in the observed DNA binding between the experimental states even if there are not differences in the amount of DNA occupancy between the experimental states. Thus, hypothesis tests are essential to assessing whether there is sufficient evidence that the difference in DNA binding reflects a true difference in DNA occupancy between experimental states. The process of performing hypothesis tests to identify statistically significant differences in the DNA binding between experimental states is called *differential binding analysis* and is also a popular tool for analyzing other types of high-throughput data beyond ChIP-Seq. For instance, Cleavage Under Targets and Release Using Nuclease (CUT&RUN) [19, 22] also leverages differential binding analysis to assess changes in protein-DNA interaction between experimental states.<sup>2</sup>

To perform biologically meaningful differential binding analysis, the raw read counts in each peak must be normalized between samples in order, since the raw read counts can be impacted by experimental artifacts, like changes in the amount of DNA loaded or the quality of the antibody used between samples. Such experimental artifacts have the potential to influence the sequencing (or read) depth (i.e., the total number of reads in the entire sample) for the entire sample [19], meaning that differences in the raw read counts for a given peak can arise between experimental states even when there is no difference in the DNA occupancy between the states. Therefore, the raw read counts are normalized between samples prior to differential binding analysis in an attempt to ameliorate the potential impacts of experimental artifacts on the identification of genomic regions as differentially bound [24].

There are various between-sample ChIP-Seq normalization methods available to researchers (e.g., Library Size [10], TMM [21], and RLE [15]). While the role of normalization methods has been analyzed through the lens of their technical conditions for RNA-seq [12], another popular method of high-throughput sequencing, there has been no parallel analysis for between-sample normalization methods for ChIP-Seq. However, ChIP-Seq and RNA-Seq data differ from each other in crucial ways. For one, RNA-Seq focuses on characterizing (differential) gene expression, while ChIP-Seq focuses on characterizing (differential) DNA occupancy. As a result, ChIP-Seq data does not have pre-defined genomic regions of interest, whereas genes serve as the genomic regions of interest in RNA-Seq data. Indeed, the genomic regions of interest in ChIP-Seq are defined through the process of *peak calling*, which leverages hypothesis testing to identify regions that are significantly enriched with DNA binding [27]. Further, because the experimental processing of ChIP-Seq samples involves many steps over multiple days, and because both antibody quality and cell number contribute to the level of background noise, the signal-to-noise ratio can be quite variable between samples in ChIP-Seq data compared to that in RNA-Seq data [13]. Hence, we cannot directly apply the results from previous RNA-Seq between-sample normalization analyses to ChIP-Seq between-sample normalization methods given the differences between RNA-Seq and ChIP-Seq data. Rather, the between-sample normalization methods for ChIP-Seq data must be explicitly analyzed through the lens of their own technical conditions.

In this article, we identify three important technical conditions underlying between-sample normalization methods for ChIP-Seq and similarly structured types of high-throughput data: **(1)** symmetric differential DNA occupancy, **(2)** equal DNA occupancy across experimental states, **(3)** equal background binding across experimental states. By simulating ChIP-Seq data, we demonstrate how violating these technical conditions can greatly impact the false discovery rate and power to detect peaks with differential DNA occupancy in downstream differential binding analysis, thereby affecting the biological conclusions drawn from ChIP-Seq

---

<sup>1</sup>In current literature, the population parameter and its sample estimate are usually both referred to as DNA binding (per cell). However, we use distinct terms in this article to disambiguate when we refer to the population parameter (DNA occupancy) or its sample estimate (DNA binding).

<sup>2</sup>CUT&RUN produces very similar data to ChIP-Seq. The difference between the techniques is that in CUT&RUN, DNA fragments are generated by adding an anti-IgG-micrococcal nuclease fusion protein after adding the primary antibody to the target of interest, rather than by sonicating the DNA as in ChIP-Seq. After binding to the primary antibody, the fusion protein cuts the DNA around the target protein, producing sequenced fragments in CUT&RUN. CUT&TAG is a variation that uses tagmentation to generate cut fragments rather than micrococcal nuclease.

experiments. We also use experimentally collected CUT&RUN data from Ashby *et al.* [2] to verify the similarities between normalization methods that we see in our simulation study since CUT&RUN data employs the same data analysis framework as ChIP-Seq to identify changes in the amount of DNA occupancy between experimental states. Our use of experimental CUT&RUN data also showcases how various normalization methods could be used to generate a ‘high-confidence’ peakset for differentially occupied regions. Ultimately, our findings underscore that satisfying the technical conditions underlying the selected normalization method is crucial for conducting biologically meaningful differential binding analysis. Therefore, we recommend that researchers use their understanding of the experiment at hand to guide their choice of ChIP-Seq between-sample normalization method when possible. Alternatively, researchers could conduct analogous data analyses in which they only vary the between-sample normalization method when there is uncertainty about which technical conditions are violated. A separate differentially bound peakset would then be generated for each between-sample normalization method. Then, the researcher could use an intersection of these peakset to create a ‘high-confidence’ peakset which is more robust to violations of the between-sample normalization technical conditions than the peakset associated with any singular between-sample normalization method, thereby limiting the impact of their choice of between-sample normalization method on the biological conclusions from their analysis.

## 2 Normalization and Differential Binding Analysis

In ChIP-Seq data analysis, between-sample normalization is performed on the *consensus peak set between experimental states*: the subset of the called peakset which are consensus peaks in at least a certain number of experimental states. For a peak to be considered a *consensus peak within an experimental state*, it must be called as a peak within at least a certain number of *replicates* (i.e., samples corresponding to the same experimental state). After the consensus peaks across experimental states have been identified, a read count matrix can be generated, where each entry corresponds to the number of reads aligned to a given consensus peak in each sample [23]. The raw read counts are then normalized between samples and sometimes also within samples to ameliorate the effect of experimental artifacts on differential binding analysis. Typically, the normalized read count for consensus peak  $i$  in sample  $j$  is computed as follows, where  $s_j$  denotes the sample-wide size factor that corresponds sample  $j$ :<sup>3</sup>

$$k_{ij}^* = \frac{k_{ij}}{s_j} \quad (1)$$

In ChIP-Seq, the overarching goal of between-sample normalization is to eliminate the differences in the read count between sample groups that are due to experimental artifacts rather than changes in the DNA occupancy between the experimental states. Experimental artifacts, such as the amount of DNA loaded into the sequencer, the quality of the antibody, the starting cell number, how many reads are returned from the sequencer, can influence how many reads are aligned to a particular genomic region within a given sample [19]. As a result, between-sample normalization is considered to have properly normalized the ChIP-Seq data between experimental states when the relationship between the samples’ normalized read counts tracks the relationship between the samples’ DNA occupancy. In other words, peaks that do not have differential DNA occupancy between samples should have the same normalized read counts across the samples, on average. In contrast, peaks that do have differential DNA occupancy between samples should have different normalized read counts across the samples under correct between-sample normalization, on average. Figure 1 demonstrates the difference between incorrect and correct ChIP-Seq between-sample normalization through a toy example (figure adapted from Evans *et al.* [12]).

---

<sup>3</sup>Some methods that we consider in this article, such as MAnorm2 and Loess Adjusted Fit (Reads in Peaks), normalize the raw reads by scaling them via (local) regression instead of scaling each read in a given sample by the same factor.

## 2.1 Importance of Proper Normalization to Differential Binding Analysis

Proper between-sample normalization is crucial for meaningful differential binding analysis. Indeed, Wu *et al.* notes that out of all the ChIP-Seq data analysis steps they analyzed, between-sample normalization has the greatest potential to influence the discovery of differentially bound regions [26]. Figure 1 walks through a toy example where a standard normalization technique (Library Size (Reads in Peaks)) does not provide the correct normalization, leading to incorrect differential binding analysis results. In the toy example, there is unequal DNA occupancy between experimental states A and B, with state B having a higher amount of total DNA occupancy than state A. Additionally, only peak 3 has differential DNA occupancy between the experimental states, with it having double the amount of DNA occupancy in state B compared to in state A. As we highlight later on, Library Size (Reads in Peaks) relies on the technical condition that there is equal DNA occupancy across the experimental states. As a result, when the read counts in the toy example are normalized via Library Size (Reads in Peaks), all three peaks appear to be differentially bound between states A and B, even though only Peak 3 has differential DNA occupancy between the states (see Figure 1(e)). The relationship between the normalized reads for Peak 3 also does not align with the relationship between the DNA occupancy for Peak 3 when Library Size (Reads in Peaks) normalization is used. Hence, the toy example in Figure 1 underscores that understanding the technical conditions of the selected between-sample normalization method and whether they are violated in a particular instance is crucial to obtaining differential binding analysis results that are biologically meaningful. In the next section, we go through several technical conditions and connect them to common ChIP-Seq between-sample normalization methods, many of which are available via *DiffBind*, an R Bioconductor package that is specifically designed for identifying differentially bound peaks between two sample groups [23].

## 3 Normalization Methods and their Technical Conditions

In this section, we identify the primary technical conditions underlying ChIP-Seq between-sample normalization methods and categorize common ChIP-seq between-sample normalization methods based on the technical conditions we identify. Before delving into the normalization methods and their respective technical conditions, though, we define two relevant terms:

1. *Reads in Peaks Normalization* methods only use reads from the consensus peakset across experimental states [23]. Figure 2 provides an illustration of the normalization unit for Reads in Peaks normalization methods.

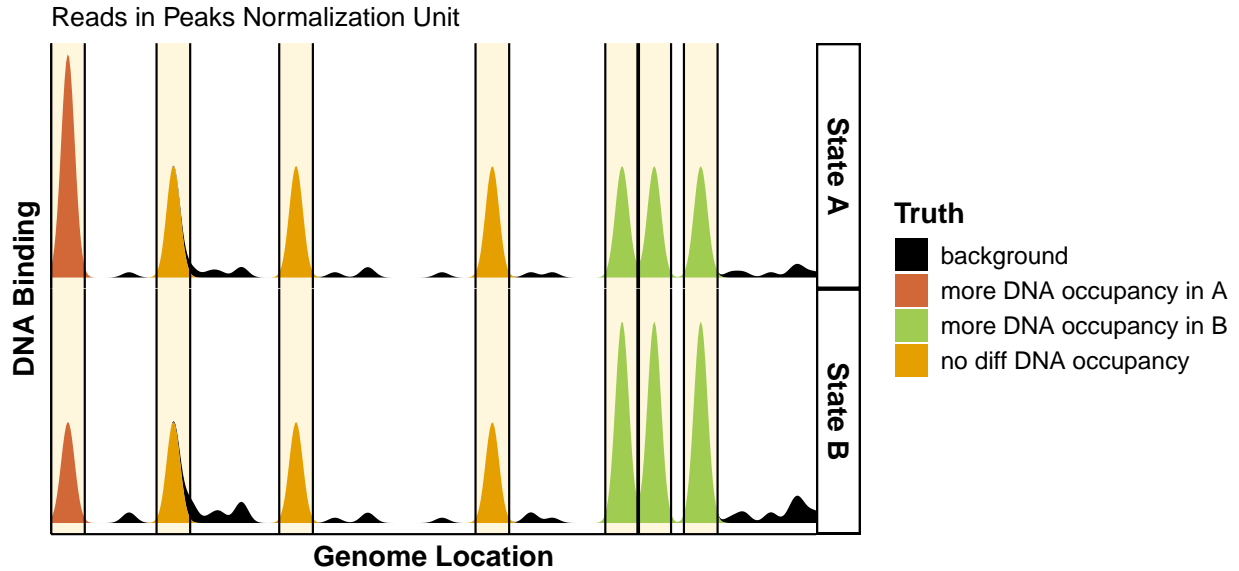


Figure 2: Reads in Peaks' normalization unit. The vertical axis represents the amount of DNA binding, and the horizontal axis represents the location of the DNA binding in the genome. The plots are faceted based on their experimental state. The genomic regions highlighted in yellow are normalization units for Reads in Peaks methods. The black vertical lines denote the boundaries of each unit. Notice only the peaks are used in Reads in Peaks normalization methods.

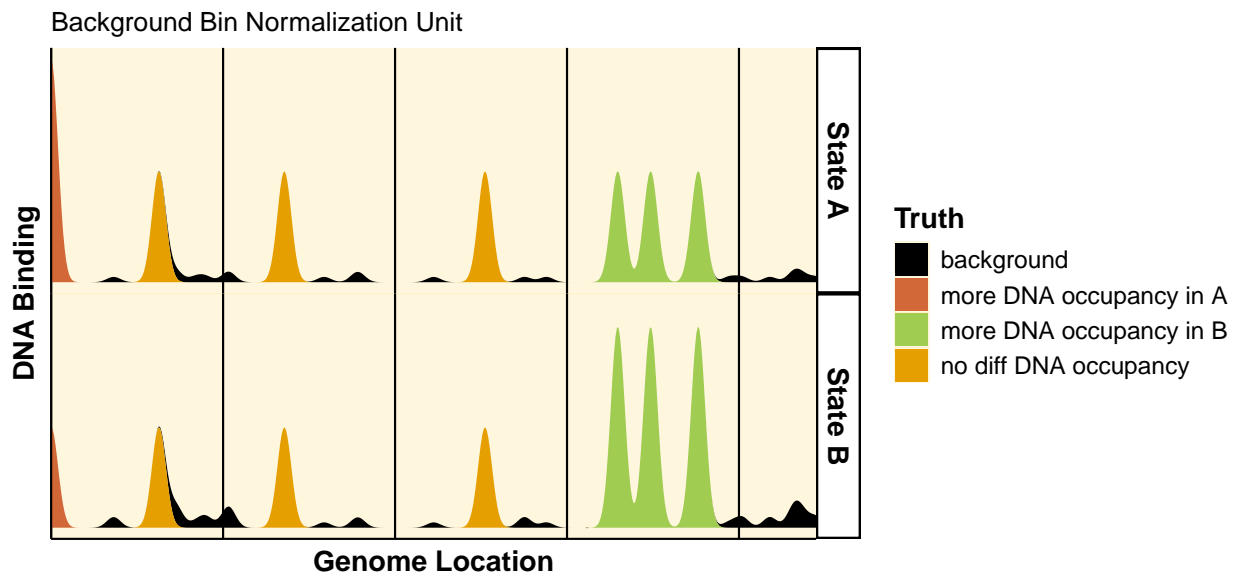


Figure 3: Background Bins' normalization unit. The vertical axis represents the amount of DNA binding, and the horizontal axis represents the genome location of the DNA binding. The plots are faceted based on their experimental state. Every genomic region highlighted in yellow would be used in Background Bins Normalization. The black vertical lines denote the boundaries of each normalization unit.

2. *Background Bins Normalization* methods partition each chromosome (that contains a peak in the consensus peakset) into roughly 15,000 base pairs long bins. These bins are used to normalize between experimental states [23]. Figure 3 provides an illustration of the normalization unit for Background Bins normalization methods.

### 3.1 Normalization by Library Size

Normalization by Library Size methods attempt to remove any differences in DNA binding that are due to experimental artifacts rather than differential DNA occupancy between samples by scaling each sample’s raw reads by the total amount of DNA binding in the sample.

#### 3.1.1 Technical Conditions

- **Equal Amount of Total DNA Occupancy:** The total amount DNA occupancy is equal across the experimental states. That is, each experimental state has the same amount of total DNA occupancy per cell (see Figure 4).

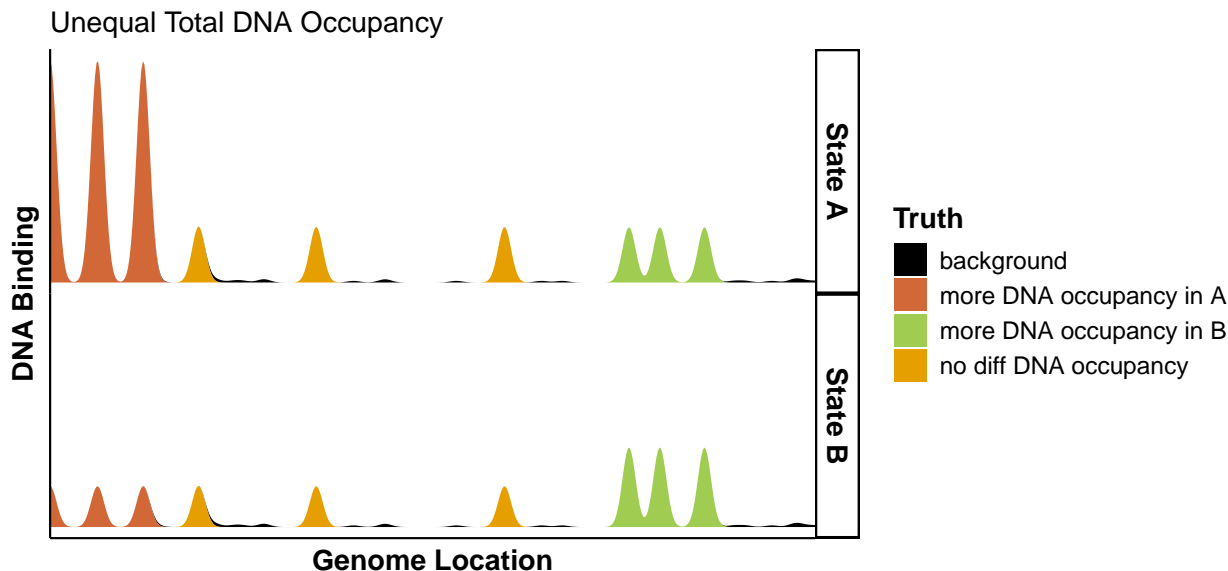


Figure 4: An illustration showing symmetric differential DNA occupancy and constant background but **unequal** total DNA occupancy across the experimental states, with state A having more total DNA occupancy than state B.

#### 3.1.2 Methods

1. **Library Size (Reads in Peaks)** first sums the raw read counts for peaks in the consensus peakset across experimental states to calculate the total number of raw reads in the peaks for the given sample. The sample is then normalized between samples by dividing the raw read count in each peak by the sample’s total raw read count in the peaks [10]. Hence, the size factor for sample  $j$  is equivalent to sample  $j$ ’s total raw peak read count under Library Size (Reads in Peaks). That is:

$$s_j = \sum_{i=1}^I k_{ij} \quad (2)$$

where  $I$  is the number of consensus peaks across the experimental states and  $k_{ij}$  is the raw read count associated with consensus peak  $i$  in sample  $j$ .

2. Library Size (Background Bins) follows a similar procedure to Library Size (Reads in Peaks) but instead sums the raw reads across all the chromosomes which contain at least one peak in the consensus peakset across the experimental states to find the samples total raw read count [23]. The raw read count associated with each peak is then divided by the sample's total raw read count in order to normalize between samples [10].
3. Loess Adjusted Fit (Reads in Peaks) is a normalization method native to *csaw*, an *R* Bioconductor package [17] that works similarly to the variant of fast linear loess introduced by Ballman *et al.* [3] and adjusts for the sample's library size and mean centering when normalizing between sample groups [23]. Loess Adjusted Fit (Reads in Peaks) works by normalizing the raw read counts via local regression on the MA values, meaning there are no sample-wide size factors calculated for Loess Adjusted Fit (Reads in Peaks). Here, the  $M$  value for a peak is the difference in the log-transformed DNA binding within the given peak across two samples, and the  $A$  value is the average log-2 binding level for that peak across the two samples [11]. Formally, the  $M$  and  $A$  values between two samples,  $j$  and  $l$ , are defined as follows for some consensus peak  $i$ :

$$M_i = \log_2(k_{ij}) - \log_2(k_{il}) \quad (3)$$

$$A_i = \frac{1}{2} \left( \log_2(k_{ij}) + \log_2(k_{il}) \right) \quad (4)$$

where  $k_{ij}$  is the raw read count associated with consensus peak  $i$  for sample  $j$ , and  $k_{il}$  is the raw read count associated with consensus peak  $i$  for sample  $l$ .

Loess Adjusted Fit (Reads in Peaks) normalization employs the following general algorithm [3]:

- (a) Construct an average array that consists of the average log-2 read counts for each consensus peak across the experimental states.
- (b) Plot a modified MA plot between the raw read counts in sample  $j$  and the average array from step (a).
- (c) Fit a loess curve on the modified MA plot.
- (d) Subtract the loess-fitted value from the relevant modified  $M$  value to compute the normalized read count estimates for sample  $j$ .
- (e) Repeat steps (b) through (d) for each sample across the experimental states.
- (f) Repeat steps (a) through (e) until the algorithm converges for each peak  $i$  and sample  $j$  across the experimental states. These converged estimates would be the normalized read counts used in downstream differential binding analysis.

Let  $\text{mean}_i(\log_2(k_i))^t$  denote the average array calculated in step (a) for the algorithm iteration  $t$ . Then, the  $M$  and  $A$  values in the modified MA plot between the sample  $j$  and the average array are computed as follows for algorithm iteration  $t$ :

$$M_i^t = \log_2(k_{ij}) - \text{mean}_i(\log_2(k_i))^t \quad (5)$$

$$A_i^t = \text{mean}_i(\log_2(k_i))^t \quad (6)$$

Next, let  $\text{loess}(\text{mean}_i(\log_2(k_i))^t)$  denote the loess-fitted value at the consensus peak  $i$  that is computed in step (c) of the normalization algorithm. For step (d), this fitted value is subtracted from  $M_i^t$  to calculate the normalized read count estimate,  $k_{ij}^{t*}$ , for peak  $i$  in sample  $j$  for algorithm iteration  $t$ :

$$k_{ij}^{t*} = M_i^t - \text{loess}(\text{mean}_i(\log_2(k_i))^t) \quad (7)$$

In step (e), the process of calculating the normalized read count estimate,  $k_{ij}^{t*}$ , is then repeated for each peak and sample across the experimental states. In step (f), the entire process (steps (a) through (e)) is repeated until the algorithm converges to a singular normalized read count estimate for each consensus peak and sample, meaning that the normalized read count for peak  $i$  in sample  $j$  for Loess Adjusted Fit (Reads in Peaks) is the following:

$$k_{ij}^* = \lim_{t \rightarrow \infty} \left( M_i^t - \text{loess}(\text{mean}_i(\log_2(k_i))^t) \right) \quad (8)$$

As explained by Lun and Smyth [17] as well as Stark and Brown [23], Loess Adjusted Fit (Reads in Peak) normalization can correct trended biases in the data, where the fold change (M values) systematically change as the average binding levels (A values) change. However, if these systematic changes are due to genuine biological signal, then normalizing the data with Loess Adjusted Fit (Reads in Peaks) could lead to peaks with differential DNA occupancy between experimental states going undetected or conversely, for peaks without differential DNA occupancy between experimental states to be identified as differentially bound during differential binding analysis [23]. Crucially, when there is unequal DNA occupancy between the experimental states, we expect there to be a systematic difference in the fold change as the average binding levels change as a result. Hence, Loess Adjusted Fit (Reads in Peaks) relies on the technical condition that there equal DNA occupancy between experimental states to properly normalize between sample groups.

### 3.1.3 Motivation for Library Methods

When there is an equal amount of total DNA occupancy between experimental states, we expect that a peak will have the same proportional share of DNA binding across the experimental states, on average. Likewise, any systematic difference in the DNA binding fold changes for different average DNA binding levels will be the result of biases in the data rather than genuine biological signal. As such, if there is an equal amount of DNA occupancy between the experimental states, then comparing the proportional share of DNA binding for a peak across the experimental states would properly normalize the data between sample groups.

## 3.2 Normalization by Distribution

Normalization by Distribution methods leverage an aspect of the raw read count distribution (or a function of it) to normalize between sample groups.

### 3.2.1 Technical Conditions

- **Symmetric Differential DNA Occupancy:** there is roughly symmetric differential DNA occupancy across the experimental states. That is, the number of peaks with more DNA occupancy (per cell) in one experimental state is approximately equal to the number of peaks with more DNA occupancy (per cell) in the other experimental state(s) (see Figure 5).
- **Peaks with Differential DNA Occupancy and Peaks without Differential DNA Occupancy Behave the Same:** the effects of any experimental artifacts on the peaks with differential DNA occupancy are the same as the effects of the experimental artifacts on the peaks without differential DNA occupancy.



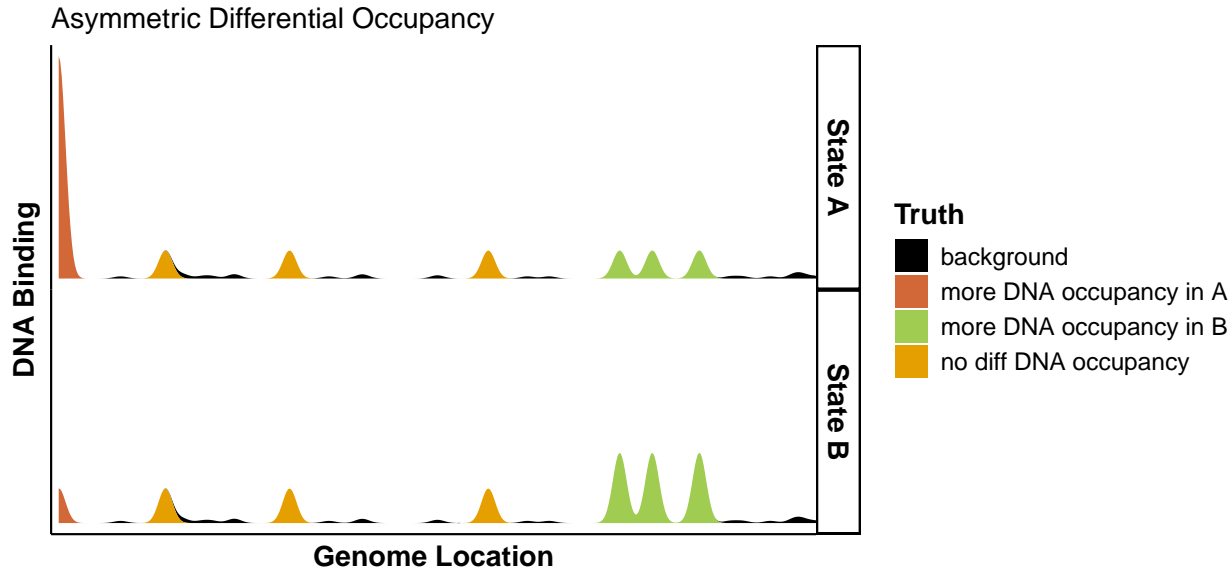


Figure 5: A toy example showing equal total DNA occupancy and constant background but **asymmetric** differential DNA occupancy across the experimental states, with state A having one peak with more DNA occupancy, and state B having three peaks with more DNA occupancy.

### 3.2.2 Methods

1. Trimmed Mean of the M-values (TMM) (Reads in Peaks) normalization first selects a sample to serve as the basis of comparison for the other samples.<sup>4</sup> Then, the M and A values of the signal magnitudes are calculated for each peak in the consensus peakset across the experimental states, relative to the selected reference sample [21].

Let  $k_{ij}$  be the raw read count associated with consensus peak  $i$  in sample  $j$ ,  $N_j$  be the total number of reads associated with the consensus peakset in sample  $j$  (i.e.,  $N_j = \sum_i k_{ij}$ ), and  $r$  be the selected reference sample. Then, the M value for consensus peak  $i$  in sample  $j$ , relative to reference  $r$ , is defined as follows:

$$M_{ij}^r = \frac{\log_2(k_{ij}/N_j)}{\log_2(k_{ir}/N_r)} \quad (9)$$

Meanwhile, the A value for peak  $i$  in sample  $j$ , relative to reference  $r$  is defined as follows:

$$A_{ij}^r = \frac{1}{2} \log_2 \left( \frac{k_{ij}}{N_j} \cdot \frac{k_{ir}}{N_r} \right) \quad (10)$$

The  $M_{ij}^r$  and  $A_{ij}^r$  values are then trimmed twice such that only peaks with central  $M_{ij}^r$  and  $A_{ij}^r$  values remain [21].<sup>5</sup> The goal of trimming the  $M_{ij}^r$  and  $A_{ij}^r$  values is to approximate a set of consensus peaks that do not have differential DNA occupancy between the experimental states. However, for trimming the non-central  $M_{ij}^r$  and  $A_{ij}^r$  values to correctly approximate a set of peaks without differential DNA occupancy, there must be a symmetric amount of differential DNA occupancy between the experimental

<sup>4</sup>TMM selects the sample whose upper quartile of DNA binding is closest to the mean upper quartile of DNA binding as the reference sample by default [8].

<sup>5</sup>By default, the  $M_{ij}^r$  values are trimmed by 30%, and the  $A_{ij}^r$  values are trimmed by 5% [21].

states. Let the set of peaks remaining after the trimming the  $M_{ij}^r$  and  $A_{ij}^r$  values as  $Q$ . The set  $Q$  is used to calculate the sample-wide size factor for sample  $j$  ( $s_j$ ), scaled by the reference sample  $r$ :

$$\log_2(s_j) = \frac{\sum_{i \in Q} w_{ij}^r M_{ij}^r}{\sum_{i \in Q} w_{ij}^r} \quad (11)$$

where,

$$w_{ij}^r = \frac{N_j - k_{ij}}{N_j k_{ij}} + \frac{N_r - k_{ir}}{N_r k_{ir}} \quad (12)$$

Notably, TMM (Reads in Peaks) calculates the sample-wide size factor for sample  $j$  only using the subset of consensus peaks in  $Q$ , i.e., the set which approximates the consensus peaks without differential DNA occupancy between experimental states. As such, TMM (Reads on Peaks) relies on the technical condition that the peaks with differential DNA occupancy behave the same as the peaks without differential DNA occupancy. Otherwise, the effects of experimental artifacts on the peaks without differential DNA occupancy would not be representative of the effects of experimental artifacts on the peaks with differential DNA occupancy.

2. Relative Log Expression (RLE) (Reads in Peaks) normalization first finds the ratio of the raw read count associated with consensus peak  $i$  in a given sample to the pseudo-reference sample, which is the geometric mean of the raw read count associated with consensus peak  $i$  across all of the samples [15]. The process of calculating the ratio between the raw read count and the geometric mean of the raw read counts is repeated until a ratio has been generated for every peak in the consensus peakset across experimental states. From here, the median ratio is computed for each sample and this median ratio serves as the sample's sample-wide size factor [15]. That is, the sample-wide size factor for some sample  $j$  ( $s_j$ ) using RLE (Reads in Peaks) normalization is defined as follows:

$$s_j = \text{median}_i \left( \frac{k_{ij}}{(\prod_{l=1}^m k_{il})^{1/m}} \right) \quad (13)$$

where  $k_{ij}$  is the raw read count associated with consensus peak  $i$  in sample  $j$  and  $m$  is the total number of samples across all the experimental states.

The purpose of using the median ratio as the sample-wide size factor is to approximate the read count for peak that does not have differential DNA occupancy between the experimental states [15]. For peaks without differential DNA occupancy between experimental states, any difference in the median ratio between would be due to experimental artifacts rather than genuine biological signal, thereby making the median ratio a meaningful sample-wide size factor. As such, RLE (Reads in Peaks) relies on the median peak not having differential DNA occupancy between the experimental states to properly normalize the data between samples. Indeed, when there is asymmetric DNA occupancy and a high proportion of peaks with differential DNA occupancy, the peak corresponding to the median ratio would have differential DNA occupancy between experimental states, making the median ratio a poor basis of normalization. Moreover, it follows that RLE (Reads in Peaks) also has the technical condition that the peaks without differential DNA occupancy behave the same as the peaks with differential DNA occupancy given that RLE (Reads in Peaks) generates each sample's size factor by approximating a ratio for a consensus peak without differential DNA occupancy between experimental states.

3. MAnorm2 is a normalization method specifically designed for ChIP-Seq data by Tu *et al.* [25]. MAnorm2 first normalizes the samples within a given experimental state. Then, the data is normalized across experimental states. Both of MAnorm2's normalization steps utilize the same general algorithm, which we describe in the subsequent paragraphs.

Let  $k_{ij}$  denote the raw read count associated with peak  $i$  in sample  $j$ . In MAnorm2, the normalized read count for peak  $i$  in sample  $j$  relative to sample  $l$ , which we denote as  $k_{ij}^*$ , is defined as follows:

$$k_{ij}^* = \alpha_j + \beta_j \cdot \log_2(k_{ij}) \quad (14)$$

Notice that MAnorm2 does not generate a sample-wide size factor for sample  $j$ . Instead, each peak’s normalized read count is a linear function of its log-2 transformed raw read count. The linear coefficients  $\alpha_j$  and  $\beta_j$  associated with sample  $j$  in Equation (14) are computed by comparing the raw read counts in the common peaks across the two samples. A peak is considered a *common peak* if it is called as a peak within both samples [25]. The coefficients  $\alpha_j$  and  $\beta_j$  in Equation (14) are defined as follows, where  $[k_j]$  is a vector with entries consisting of the raw read count associated with common peak  $i$  in sample  $j$ , and  $sd_i$  denotes the sample estimate of the standard deviation in the raw read counts across the common peaks  $i$  within sample  $j$ :

$$\alpha_j = \text{mean}_i \left( \log_2([k_l]) - \beta_j \cdot \text{mean}_i(\log_2([k_j])) \right) \quad (15)$$

$$\beta_j = \frac{sd_i(\log_2([k_l]))}{sd_i(\log_2([k_j]))} \quad (16)$$

Let  $[M^*]$  denote the vector of the normalized M values in the common peak regions across samples  $j$  and  $l$ , and  $[A^*]$  denote a vector of the normalized A values in the common peak regions across samples  $j$  and  $l$ . Then,  $[M^*]$  and  $[A^*]$  are computed as follows, where  $[k_j^*]$  is a vector consisting of the normalized read counts in sample  $j$  associated with each peak  $i$  (i.e.,  $k_{ij}^*$ ), and  $k_l$  is a vector consisting of the raw read counts associated with sample  $l$  for each peak  $i$ :

$$[M^*] = [k_j^*] - \log_2([k_l]) \quad (17)$$

$$[A^*] = \frac{1}{2} \left( \log_2([k_l]) + [k_j^*] \right) \quad (18)$$

Based on how  $\alpha_j$  and  $\beta_j$  are defined, the  $[M^*]$  and  $[A^*]$  vectors associated with the two samples will satisfy the following two conditions under MAnorm2 normalization:

$$\text{mean}_i([M^*]) = 0 \quad (19)$$

$$\text{cov}_i([M^*], [A^*]) = 0 \quad (20)$$

Equations (19) and (20) guarantee that the ordinary least squares line on the normalized MA plot is the horizontal axis. When there is asymmetric differential occupancy between experimental states, the ordinary least squares line on the raw MA plot is skewed towards the experimental state with more differential DNA occupancy per cell, which is to say that the raw M-values will be more extreme for the states with higher DNA occupancy. In turn, when the read counts are normalized such that Equations (19) and (20) are satisfied, the normalized M values associated with peaks that do not have differential DNA occupancy between states will be pulled away from zero (on the log-2 scale) to offset the asymmetric distribution of the M values, thereby leading to false discoveries of differentially bound peaks. Therefore, MAnorm2 relies on the technical condition that there is symmetric differential DNA occupancy between experimental states.<sup>6</sup>

---

<sup>6</sup>In the original paper introducing MAnorm2, Tu *et al.* note that MAnorm2 assumes that there is “no global change of protein binding intensities” in the common peak regions [25]. From our understanding of the method’s details, they are describing symmetric differential occupancy rather than an equal total amount of DNA occupancy in this statement.

### 3.2.3 Motivation for Distribution Methods

Normalization by Distribution methods work by supposing that we can normalize the raw read counts by comparing characteristics of the read count distribution between samples. If most peaks do not have differential DNA occupancy between the experimental states, then the central measurements of the raw read count distribution will correspond to a peak without differential DNA occupancy between states. Additionally, if the effects of experimental artifacts on the peaks that have differential DNA occupancy are the same as the effects of experimental artifacts on the peaks that do not have differential DNA occupancy, then we can properly normalize the entire sample by using the sample-wide size factor that we computed by approximating a peak *without* differential DNA occupancy between the experimental states.

## 3.3 Normalization by Background

Normalization by Background methods first partition the chromosomes into background bins that are roughly 15,000 base pairs long [23]. For Normalization by Background methods, the background bins rather than the consensus peakset serve as the normalization unit (see Figure 3).

### 3.3.1 Technical Conditions

- Equal Amount of Background Binding: the number and distribution of rogue reads (i.e., binding in regions that are not truly occupied by the protein of interest) within each sample is roughly the same across the experimental states.
- Previous Technical Conditions: the aforementioned technical conditions for any given method must be met by the background bins across the experimental states. Because the background has zero differential occupancy (by definition), when using bins as normalization units, the technical conditions must be met when describing the DNA binding across the background bins.

### 3.3.2 Methods

1. Library Size (Background Bins) was previously described in the Normalization by Library Size methods section. To summarize: a sample is normalized using Library Size (Background Bins) by dividing the raw read count associated with each peak by the total raw read count summed over the background bins [10].
2. Trimmed Mean of the M-Values (TMM) (Background Bins) or works very similarly to TMM (Reads in Peaks). The key difference is that the unit used to generate the sample-wide size factor is the background bins rather than the consensus peakset across experimental states for TMM (Background Bins).
3. Relative Log Expression (RLE) (Background Bins) uses the same normalization procedure as RLE (Reads in Peaks), but, like with TMM (Background Bins), the background bins are used to generate the sample-wide size factor rather than the consensus peakset across experimental states for RLE (Background Bins).

### 3.3.3 Motivation for Background Methods

Peaks are typically only a few hundred base pairs long. So, any substantial (non-trivial) difference in the amount of DNA binding in a given background bin across experimental states is expected to be the result of different experimental artifacts between samples rather than true biological differences in the amount of DNA occupancy between experimental states [23]. Thus, we can leverage background bin methods to properly normalize between samples, insofar as the technical condition that there is an equal amount of background binding across experimental states is satisfied.

### 3.4 Normalization by Spike-in DNA

When experimental data violates the technical conditions listed in the previous sections, Normalization by Spike-in DNA can enable us to properly normalize between ChIP-Seq samples. Normalization by Spike-in DNA works by amending the ChIP-Seq data collection procedure, by adding a fixed amount of DNA from an organism that is not interrogated in the experiment prior to immunoprecipitation. For example, in a ChIP-Seq experiment using mammalian cells, yeast DNA could be added. The assumption is that any yeast DNA that remains in the final sample represents background, since none of the yeast DNA would be occupied by the mammalian protein of interest. Figure 6 provides a toy example that compares the experimental ChIP-Seq data with the data generated from spike-in controls.

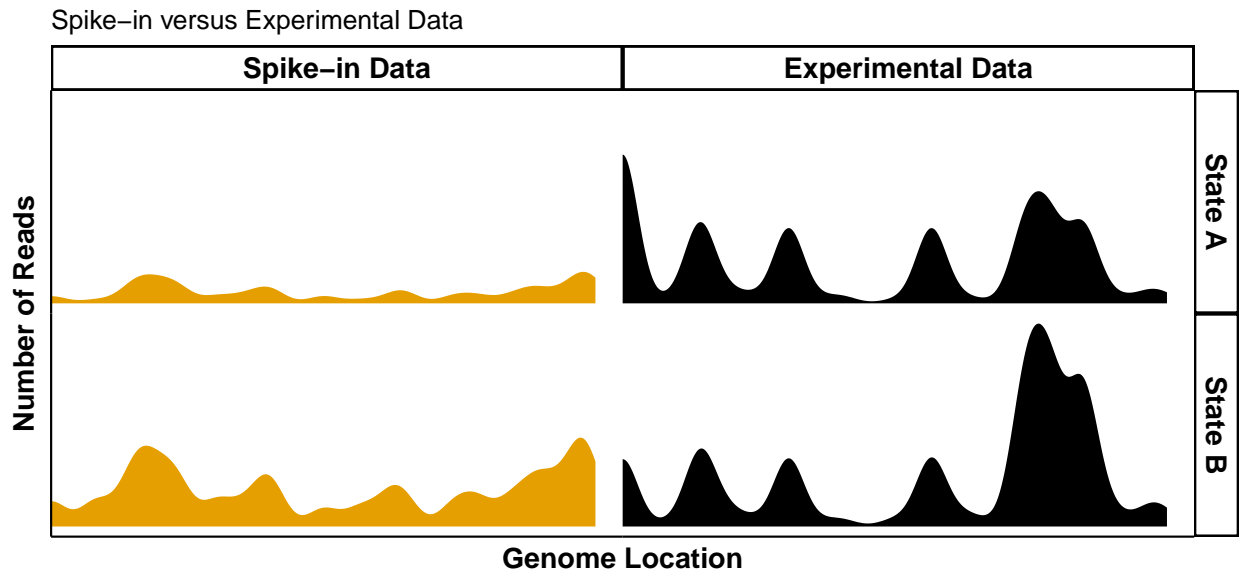


Figure 6: Spike-in Control Illustration. The horizontal axis is the genome location, and the vertical axis is the number of reads aligned to that genome location. The plot is faceted by spike-in versus experimental data as well as by experimental state (A versus B). The left side of the plot (in yellow) corresponds to the spike-in DNA data. Note how there are no sharp peaks in the spike-in data since there should be no changes in DNA occupancy within the spike-in control samples. In contrast, there are sharp peaks on the right side of the plot (in black), which corresponds to the experimental data. Note that there are more reads in the spike-in control data for State B than State A (compare the right plots). Normalization with spike-in DNA would aim to eliminate the discrepancy between the spike-in sample read counts across the two States.

#### 3.4.1 Technical Conditions

- Existence of Spike-in Controls: the spike-in DNA was added by the experimenter, and it comes down in the immunoprecipitation with the same frequency regardless of the experimental state.
- Spike-in Controls Behave like Samples of Interest: the effects of experimental artifacts on the spike-in DNA reflect the effects of experimental artifacts on the experimental samples.

#### 3.4.2 Method

1. Normalization by Spike-in DNA works by adding in the spike-in DNA prior to immunoprecipitation [7]. If the same amount of spike-in DNA is added to each sample, then the total number of reads is expected to be the same across the samples, too [6]. Thus, any difference in the total number of reads

Table 1: Summary of the eight unique simulation conditions.

Symmetry	Equal Occupancy	Equal Background	% Peaks with More Occ. (A)	% Peaks with More Occ. (B)	FC (A)	FC (B)	Avg. % More Background/Rep <sup>1</sup>
✓	✓	✓	50	50	2	2	0
✓	X	✓	50	50	4	2	0
X	✓	✓	12.5	87.5	2	2	0
X	X	✓	12.5	12.5	8	2	0
✓	✓	X	50	50	2	2	20
✓	X	X	50	50	4	2	20
X	✓	✓	12.5	87.5	2	2	20
X	X	✓	12.5	12.5	8	2	20

The experimental state with more background binding per replicate is chosen at random in each simulation iteration. FC = fold change in DNA occupancy when comparing non-differentially occupied peaks to peaks with more DNA occupancy in the given state. Occ. = DNA Occupancy.

across spike-in control samples is taken to be the result of differences in the experimental artifacts between the samples. So, sample-wide size factors for each sample can be calculated by equalizing the spike-in signal between samples [6]. Since the spike-in DNA is not expected to have any differential DNA occupancy between states, a Normalization by Background method is used to calculate sample-wide size factors for each sample [23]. The sample-wide size factors calculated using the spike-in DNA are then applied to the relevant experimental sample in order to ameliorate the impact of experimental artifacts on the read count differences between experimental samples.

### 3.4.3 Motivation for using Spike-in DNA

We often have an a priori understanding that the amount of spike-in DNA that comes down in immunoprecipitation should remain the same across experimental states [7]. So, if the amount of spike-in DNA at a particular genomic location misaligns with this expectation, we can take this misalignment to be the result of differences in the experimental artifacts between the samples rather than genuine differences in biological signal. Moreover, assuming that the impact of experimental artifacts in the spike-in controls samples reflects the impact of experimental artifacts in the experimental samples of interest, we can apply the sample-wide size factors calculated from the spike-in DNA to the relevant experimental sample to properly normalize the experimental data between samples.

## 4 Simulations

To demonstrate the importance of satisfying technical conditions of the selected between-sample normalization method on downstream differential binding analysis, we simulate ChIP-Seq read count data across two experimental states under eight distinct conditions. Our ChIP-Seq read count data simulation builds on code from Lun and Smyth [16] as well as from Evans *et al.* [12]. The code for the ChIP-Seq simulations, result plots, experimental data analysis, and all toy examples is available in a GitHub repository.<sup>7</sup>

### 4.1 Simulation Details

In total, we simulate eight distinct conditions, which we summarize in Table 1. The eight simulation conditions are all possible combinations of (not) violating the three primary technical conditions that we

<sup>7</sup><https://github.com/scolando/ChIP-Seq-norm>

previously described: symmetric differential DNA occupancy, equal DNA occupancy across experimental states, and equal background binding across experimental states.

In our simulations, we simulate the occupancy of simple transcription factors, which typically generate narrower and taller peaks than other types of proteins which might be of interest in ChIP-seq experiments, like histone modifications [16]. Each simulation has two experimental states (denoted A and B) and four replicates per experimental state (see Appendix for results with 10 replicates per experimental state). We simulate 10,000 peaks within each replicate and vary the proportion of these peaks with differential DNA occupancy from 0.05 to 0.95, using a step size of 0.05.

Following the work of Anders and Huber [1], Evans *et al.* [12], as well as Lun and Smyth [16], we simulate the read counts associated with each peak to follow a negative binomial distribution, parameterized by the mean and dispersion. The mean of the negative binomial corresponds to the average amount of DNA binding for that genomic region within the given replicate. Like Lun and Smyth [16], the dispersion for is derived by sampling from an inverse chi-square distribution with degrees of freedom set to 10. After the read counts are generated for each peak, we then perform peak calling using MACS2 [27]. The consensus peakset across experimental states is identified using DiffBind [23], implementing a cut-off of 75% within each experimental state (i.e., a peak must be in at least 75% of replicates within a given experimental state for it to be classified as a consensus peak within the state) and then taking the union of the consensus peaks within each experimental state. Then, between-sample normalization and differential binding analysis are both performed using DiffBind (for all normalization methods except for MAnorm2) or MAnorm2 (for the MAnorm2 normalization). For normalization methods available in DiffBind, we use DESeq2 for differential binding analysis. Meanwhile, we use the differential binding analysis method that was specifically developed in conjunction with MAnorm2’s normalization method for the MAnorm2-normalized read counts [25]. For all differential binding analysis procedures, we use a false discovery rate threshold of 0.05 on the Benjamini-Hochberg adjusted p-values [5]. We repeat this entire process one hundred times for every combination of simulation condition and proportion of peaks with differential DNA occupancy, generating one hundred independent datasets.

We analyze the performance of each between-sample normalization method on the simulated data via three metrics: the average false discovery rate (FDR), average power, and the average absolute size factor ratio relative to the Oracle. The Oracle is an omniscient normalization method that calculates the correct sample-wide size factors based on the population-level simulation parameters in the negative binomial model (we describe the Oracle in more detail in the Appendix). Under ideal circumstances, correct normalization means that all and only peaks with differential DNA occupancy between experimental states are classified as differentially bound. Though, peaks could be classified as differentially bound even though it does not have differential DNA occupancy due to other steps in the data analysis workflow besides between-sample normalization. For example, a peak with differential DNA occupancy might not be called as a peak during peak calling due to low signal. Alternatively, differential binding analysis might generate a high adjusted p-value for a peak with differential DNA occupancy even though it does have different normalized read counts between samples. Therefore, given that a between-sample normalization method might still be performing well even if it corresponds to a high average FDR or a low average power, the Oracle normalization method will serve as the basis of comparison for the other normalization methods in our simulation.

We directly compare the Oracle’s sample-wide size factors to other between-sample normalization method’s through the absolute size factor ratio relative to the Oracle. We calculate the average absolute size factor ratio by first computing the absolute ratio of a method’s size factor to the Oracle’s size factor which corresponds to the same replicate.

Let  $s_{jz}$  denote the sample-wide size factor corresponding to sample  $j$  for normalization method  $z$ , and  $s_{jo}$  denote the sample-wide size factor corresponding to sample  $j$  for the Oracle. Then, the absolute size factor ratio, which we denote as  $(\text{ratio})_{jz}$ , is defined by the following piecewise function:

$$(\text{ratio})_{jz} = \begin{cases} \frac{s_{jz}}{s_{jo}} & \text{if } \frac{s_{jz}}{s_{jo}} \geq 1 \\ \frac{s_{jo}}{s_{jz}} & \text{otherwise} \end{cases} \quad (21)$$

The average absolute size factor ratio relative to the Oracle for normalization method  $z$  (i.e.,  $(\text{aasfro})_z$ )

for a given simulation condition is then defined as the mean of the absolute size factor ratios for normalization method  $z$  relative to the Oracle across all  $n$  samples:

$$(\text{aasfro})_z = \frac{1}{n} \cdot \sum_{j=1}^n (\text{ratio})_{jz} \quad (22)$$

We use the metric, along with the average FDR and power, to evaluate our simulation results in the following section.

## 4.2 Simulation Results

From Figure 7, we see that when the technical conditions of a normalization method are violated, the average FDR *increases* (i.e., that there is a higher proportion of the peaks that are identified as differentially bound do not have true differential DNA occupancy between the experimental states).<sup>8</sup> For example, the last two columns of Figure 7 show that Normalization by Distribution methods – TMM (Reads in Peaks), RLE (Reads in Peaks), and MA<sub>norm2</sub> – all do a poor job of controlling the average FDR at the threshold of 0.05 when there is the technical condition of symmetric differential DNA occupancy is violated. Meanwhile, when there is symmetric differential occupancy between the experimental states (see the first two columns in Figure 7), the Normalization by Distribution methods are able to control the average FDR at a level of 0.05, tracking closely to the Oracle. Similarly, Normalization by Library Size methods have an increased average FDR when there is unequal DNA occupancy between the experimental states, diverging from the Oracle’s average FDR, but these methods track closely to the Oracle with respect to the average FDR when the technical condition of equal DNA occupancy between experimental states is met. Finally, Normalization by Background methods are affected both by unequal background binding and unequal DNA occupancy between experimental states. We posit that unequal DNA occupancy impacts the average FDR of Normalization by Background methods because there is likely to be unequal binding in the background bins when there is there is unequal DNA occupancy along with a high proportion of peaks having differential DNA occupancy between states (see Figure 3).

Figure 8 demonstrates that normalization method performance also tends to decrease when its technical conditions are violated with respect to the average power. The decrease in the average power indicates that peaks with differential DNA occupancy are generally less likely to be identified as differentially bound when the technical conditions that underlie the normalization method are violated. For example, we see that the average power is dramatically lower for the Normalization by Distribution methods when there is asymmetric differential occupancy between the experimental states (compare the first two columns and the last two columns in Figure 8), indicating that these methods often fail to identify differentially occupied peaks as differentially bound (i.e., there is low sensitivity) when there is asymmetric differential DNA occupancy. However, the decrease in the average power when the a normalization method’s technical conditions are violated is not a universal trend. Normalization by Library Size methods maintain a high power even when the underlying technical condition of equal total DNA occupancy between experimental states is violated. Coupled with the high average FDR we see in Figure 7, this high average power indicates that Normalization by Library Size methods are *over-calling* peaks as differentially bound, on average (i.e., there is low specificity).

In the subsequent subsections, we delve deeper into how violating each of the three technical conditions affects the performance of the normalization methods, as measured by our three simulation metrics. In particular, we show how violating a normalization method’s technical conditions leads to improper between-sample normalization and ultimately the misidentification of peaks with differentially DNA occupancy between the experimental states.

---

<sup>8</sup>n.b., the average false discovery rate naturally decreases as the proportion of peaks with differential DNA occupancy increases as there are fewer peaks to falsely discover as differentially bound.



#### 4.2.1 All Technical Conditions Met

Per Figure 9, when the primary three technical conditions are met, all the normalization methods track closely to the Oracle with respect to the average FDR and power. Interestingly, the average sample-wide size factors corresponding to the Normalization by Background methods – RLE (Background Bins), TMM (Background Bins), and Library Size (Background Bins) – are different from the Oracle’s even when all three of the primary technical conditions are met, with an average absolute size factor ratio relative to the Oracle of approximately 1.15. Given these methods all control the average FDR and exhibit high power, we posit the difference in the average size factors for Normalization by Background methods to be the result of the these methods using background bins rather than peaks as the between-sample normalization unit.

#### 4.2.2 Effect of Asymmetric Differential DNA Occupancy

However, when the technical condition of symmetric differential DNA occupancy between states is violated (while the other two technical conditions are still met), the Normalization by Distribution methods diverge from the Oracle across all three metrics. From the leftmost plot in Figure 10, we see RLE (Reads in Peaks), TMM (Reads in Peaks), and MAnorm2 do a poor job of controlling the average false discovery rate relative to the FDR threshold of 0.05, particularly as the proportion of peaks with differential DNA occupancy increases. One explanation for this is that the median (and mean) peak is more likely to have differential DNA occupancy between experimental states when the proportion of peaks with differential expression increases. So, a central measure of the read count in peaks would correspond to a peak with differential DNA occupancy. As a result, the average size factors associated with RLE (Reads in Peaks) and TMM (Reads in Peaks) also diverge from the Oracle’s as the proportion of peaks with differential DNA occupancy increases (see rightmost plot of Figure 10) (since MAnorm2 does not generate sample-wide size factors, it is not depicted in the rightmost plot in Figure 10). The average power associated with the normalization by distribution methods – RLE (Reads in Peaks), TMM (Reads in Peaks), and MAnorm2 – is also much lower than the Oracle’s, with the average power falling below 25% as the proportion of peaks with differential DNA occupancy increases, while the Oracle’s average power remains near 75% (see the middle plot in Figure 10).

The Normalization by Background and Normalization by Library Size methods still track closely to the Oracle with respect to average FDR and power even with there is asymmetric differential DNA occupancy between states, which confirms that only Normalization by Distribution methods rely on there being symmetric differential DNA occupancy between experimental states to properly normalize between sample groups.

Simulation Results: Asymmetric Differential DNA Occupancy

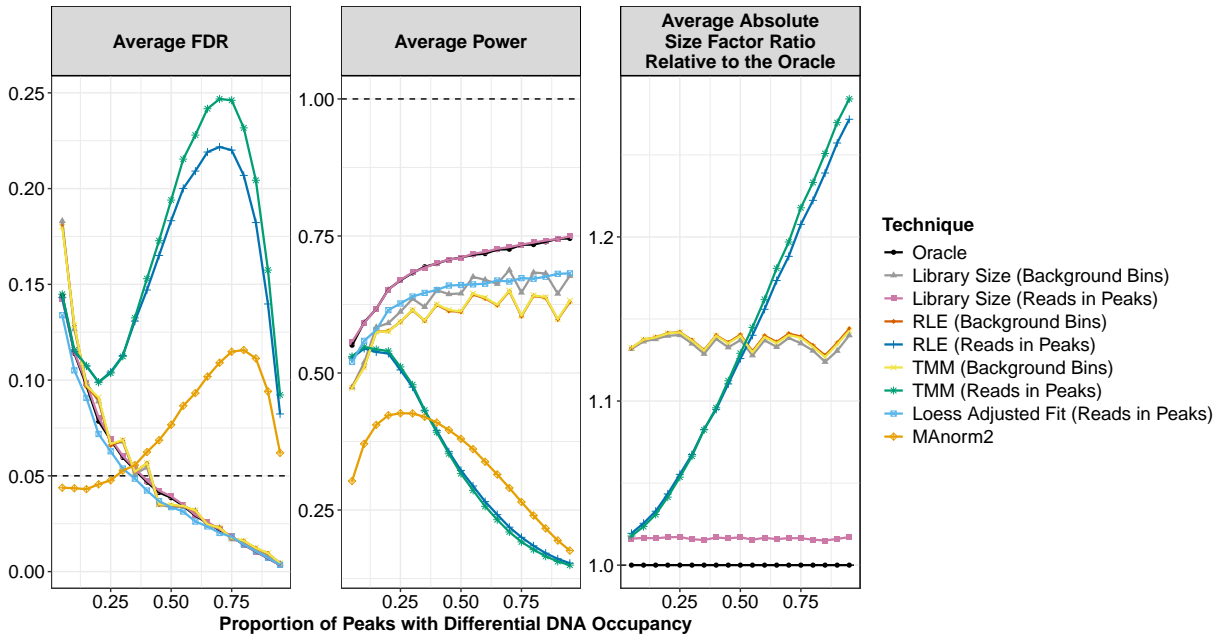


Figure 10: Simulation results when only symmetric differential is violated, with four replicates per experimental state. The horizontal axis is the proportion of peaks with differential DNA occupancy, and the vertical axis is the value for each simulation metric. The figure is faceted such that each subplot represents one of the three simulation metrics (note the scale change between each facet in the figure). The leftmost plot is the average false discovery rate, where the horizontal black line represents the 0.05 FDR threshold we set. The middle plot is the average power, where the horizontal black line at 1 represents the highest possible average power. The rightmost plot is the average absolute size factor ratio relative to the Oracle, where the horizontal line at 1 represents the Oracle’s average absolute size factor ratio with itself. Thus, a normalization method is taken to track closely with the Oracle if its curve is close to the horizontal black line at 1 in the rightmost plot. Recall that MANorm2 and Loess Adjusted Fit (Reads in Peaks) do not generate sample-wide size factors, and so do not have curves in the rightmost plot of the figure.

#### 4.2.3 Effect of Unequal Total DNA Occupancy

In contrast, Normalization by Library and Normalization by Background both fail when there is an unequal total amount of DNA occupancy between experimental states (but the other two technical conditions hold). Specifically, TMM (Background Bins), Library Size (Background Bins), RLE (Background Bins), Library Size (Reads in Peaks), and Loess Adjusted Fit (Reads in Peaks) all do a poor job of controlling the average FDR at the cut-off of 0.05 when there is an unequal amount of total DNA occupancy between the experimental states (see the leftmost plot of Figure 11) and diverge from the Oracle with respect to the average FDR. While average absolute size factor ratio relative to the Oracle increases for all normalization methods as the proportion of peaks with differential DNA occupancy increases, Normalization by Background methods uniformly have the highest average absolute size factor ratio relative to the Oracle (see the rightmost plot in Figure 11) (since Loess Adjusted Fit (Reads in Peaks) does not generate sample-wide size factors, it is not depicted in the rightmost plot in Figure 10). One explanation for this is that when the proportion of peaks with differential occupancy increases so does the difference in the amount of DNA binding in the background bins across the experimental states. As a result, the Normalization by Background bins continue to diverge farther from the Oracle’s and their average size factors are already different to begin with due to using a different normalization unit than the Oracle. Despite the Normalization by Library Size and Normalization by Background methods performing poorly with respect to the average FDR and absolute size factor ratio

relative to the Oracle, these methods retain high average power (see the middle plot of Figure 11). The high power coupled with the high average FDR indicates that Normalization by Background and Normalization by Library Size methods are over-calling peaks as differentially bound when they do not actually have differential DNA occupancy between the experimental states (i.e., lead to low specificity).

Unlike with asymmetric differential occupancy, the Normalization by Distribution methods track closely to the Oracle across all three metrics, indicating that Normalization by Distribution methods do not rely on the technical condition of equal total DNA occupancy between experimental states to properly normalize between samples.

#### 4.2.4 Effect of Unequal Background Binding

Normalization by Background methods perform the worst across all three metrics there is unequal background binding between experimental states (but the other two technical conditions are met). That is, they have the highest average FDR, lowest average power, and largest average absolute size factor ratio relative to the Oracle (see Figure 12). Still, the average absolute size factor ratio relative to the Oracle is roughly constant for TMM (Background Bins), RLE (Background Bins), and Library Size (Background Bins) even as the proportion of peaks with differential DNA occupancy increases (see the rightmost plot of Figure 12). Since the average absolute size factor ratio relative to the Oracle remains roughly constant as the proportion of peaks with differential DNA occupancy while the average FDR decreases, we postulate that average FDR is decreasing for Normalization by Background methods due to there are fewer peaks to falsely discover as differentially bound rather than these methods becoming better when the proportion of peaks with differential DNA occupancy increases.

Conversely, Normalization by Library Size and Normalization by Distribution track closely with the Oracle across all three metrics, demonstrates that these normalization methods do not rely on there being equal background binding across experimental states for proper between-sample normalization.

Simulation Results: Unequal Background Binding

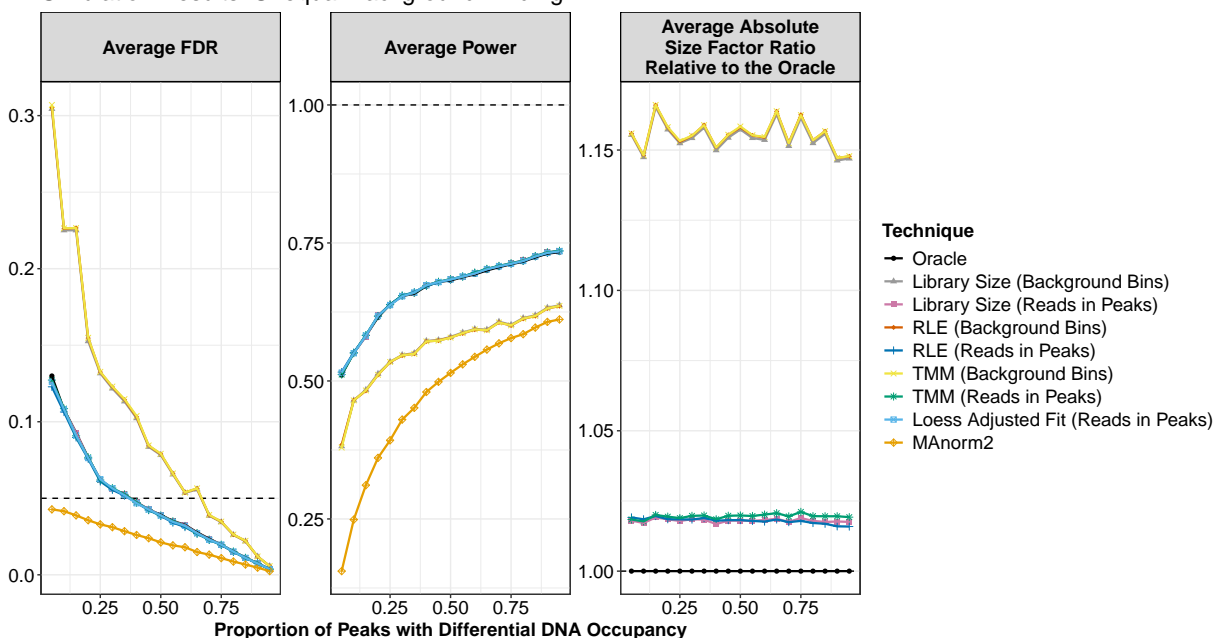


Figure 12: Simulation results when only equal background binding between experimental states is violated, with four replicates per experimental state. The horizontal axis is the proportion of peaks with differential DNA occupancy, and the vertical axis is the value for each simulation metric. The figure is faceted such that each subplot represents one of the three simulation metrics (note the scale change between each facet in the figure). The leftmost plot is the average false discovery rate, where the horizontal black line represents the 0.05 FDR threshold we set. The middle plot is the average power, where the horizontal black line at 1 represents the highest possible average power. The rightmost plot is the average absolute size factor ratio relative to the Oracle, where the horizontal line at 1 represents the Oracle’s average absolute size factor ratio with itself. Thus, a normalization method is taken to track closely with the Oracle if its curve is close to the horizontal black line at 1 in the rightmost plot. Recall that MAnorm2 and Loess Adjusted Fit (Reads in Peaks) do not generate sample-wide size factors and so do not have curves in the rightmost plot of the figure.

## 5 Experimental Results

To compare the between-sample normalization methods with data from a biological experiment, we analyze a dataset generated from the eukaryotic protozoan parasite *Trypanosoma brucei*. The dataset was generated by endogenously tagging a chromatin interacting bromodomain protein (Bdf3) with hemagglutinin (HA) and performing CUT&RUN using an anti-HA antibody [2, 18] to investigate whether Bdf3 chromatin occupancy changes as parasites transition from the mammalian bloodstream phase of the life cycle to the procyclic gut stage found in the parasite tsetse fly vector. Samples were harvested from bloodstream parasites and from several timepoints thereafter to produce the data. Previous analysis by Ashby *et al.* shows that occupancy of Bdf3 is altered at hundreds of sites as parasites transition from bloodstream to procyclic forms by generating a ‘high-confidence’ differentially bound peakset using Library Size (Spike-in), RLE (Background Bins), RPKM, and RLE (Spike-in) normalization methods [2] (the Fastq files were deposited in the SRA database under project number PRJNA795567).<sup>9</sup> To provide a simple comparison of between-sample normalization methods applicable to ChIP-Seq and similar types of data, like CUT&RUN, we examine the similarity in the log-

<sup>9</sup><https://www.ncbi.nlm.nih.gov/sra/?term=PRJNA795567>

2 fold changes after between-sample normalization (i.e., the normalized log-2 fold changes) between the bloodstream parasites and those that had been induced to transition into procyclic forms by the 3 hour mark. The 3 hour mark serves as our comparison point as it is when the greatest change in DNA occupancy is observed compared compared to the bloodstream samples [2].

We use MACS2 to conduct peak calling on each replicate, identifying 629 peaks as part of the consensus peakset across the two experimental states. We then implement ten between-sample normalization methods on the ten different copies of data via Diffbind. We use all of the same between-sample normalization methods as we do in our simulation with the exception of MAnorm2 as MAnorm2 performs both within-sample and between-sample normalization, making the MAnorm2-generated fold changes between experimental states not directly comparable to those generated by the other normalization methods which only perform between-sample normalization. Next, we test for differential binding via DESeq2 [15] in DiffBind, using the Benjamini-Hochberg adjusted p-values and an FDR threshold of 0.05.

We compare the normalized log-2 fold changes for each between-sample normalization method using Principal Component Analysis (PCA) (Figure 13) and an UpSet plot of the differentially bound peaksets generated after using each between-sample normalization method (Figure 14). Given that we cannot display every possible distinct intersection of the ten differentially bound peaksets, the UpSet plot in Figure 14 only provides information on the largest groups of distinct overlaps between the differentially bound peaksets.

Figure 13 demonstrates that the first principal component, which explains 99.45% of the variability in the normalized log-2 fold changes, primarily distinguishes methods which use reads in peaks from Normalization by spike-in DNA and Normalization by Background methods. Meanwhile, the second principal component, which explains 0.39% of the remaining variability in the normalized log-2 fold changes, separates the Normalization by Background methods from the Normalization by Spike-in DNA. The Reads in Peaks normalization methods are composed of the methods we classified as Normalization by Library Size and Normalization by Distribution in Section 3 and, as a result, many of the reads in peaks methods have shared technical conditions and thus follow similar trends in our simulation results. For example, Loess Adjusted Fit (Reads in Peaks) and Library Size (Reads in Peaks) are the most similar to each other with respect to normalized log-2 fold changes between states based on Figure 13 and also behave similarly to each other in our simulation (see Figure 4.2.3). These two methods rely on the same technical condition that there is an equal amount of total DNA occupancy across the experimental states to properly normalize between states. Additionally, the Normalization by Background methods have similar normalized log-2 fold changes based on their location in Figure 13 and all rely on the technical condition that there is a roughly equal amount of background binding across the experimental states. Indeed, the Normalization by Background methods all perform poorly when there is an unequal amount of background binding across states in our simulation (see Figure 4.2.4). Therefore, Figure 13 shows that between-sample normalization methods with the same technical conditions tend to generate more similar log-2 fold changes after between-sample normalization than methods which rely on different technical conditions, verifying our simulation findings.

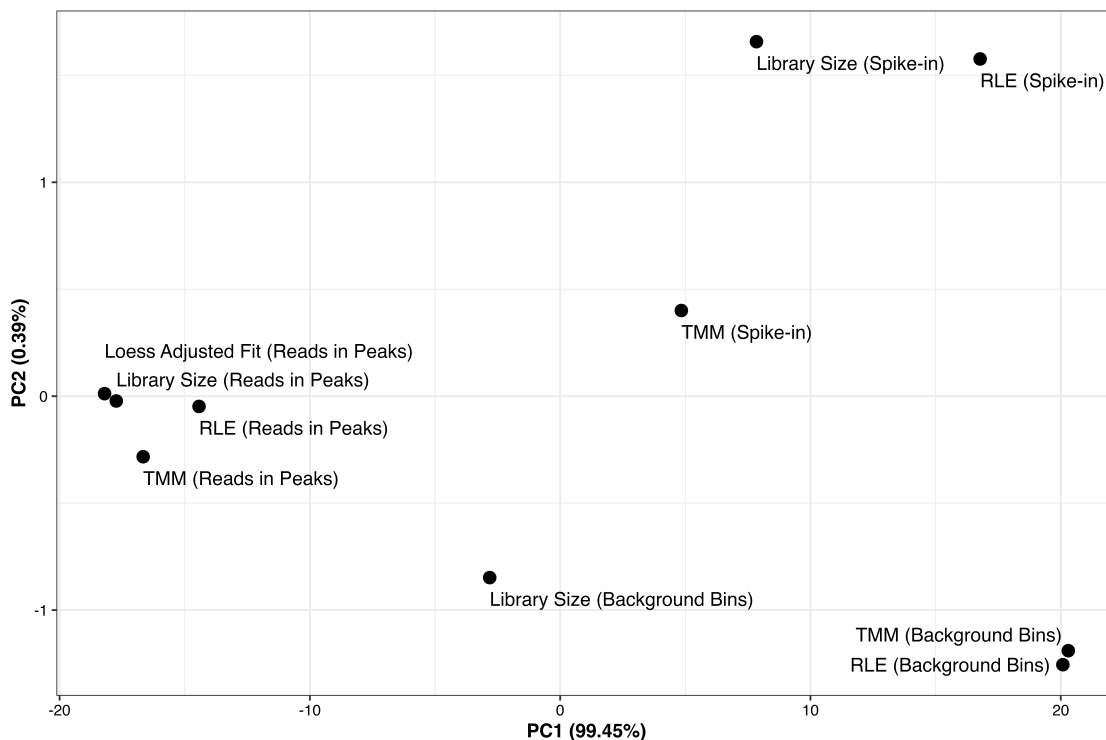


Figure 13: PCA of the log-2 fold changes after between-sample normalization across the bloodstream parasites and those induced to transition into procyclic forms by the 3 hour for each consensus peak. The horizontal axis corresponds to the first principal component, and the vertical axis corresponds the second principal component. Almost all the variability in the log-2 fold changes after between-sample normalization is explained by the first principal component (99.45%) and 0.39% of the remaining variability is explained by the second principal component. The first principal component primarily separates normalization by distribution methods from spike-in and background bin normalization methods. The second principal component distinguishes the background bin normalization methods from the spike-in normalization methods.

Figure 14 shows that 170 peaks were identified as differentially bound across the ten normalization methods between the bloodstream samples and 3 hour timepoint. These 170 peaks would constitute a ‘high-confidence’ peakset because they were found to have differential DNA binding between the 3 hour mark and the bloodstream state, regardless of which between-sample normalization method was used on the data. As emphasized by Ashby *et al.*, using a ‘high-confidence’ peakset to characterize differential DNA occupancy circumvents the problem of the one’s choice of between-sample normalization method having an “outsized effect” on which regions are identified as differentially bound between experimental states [2, 23] since a ‘high-confidence’ peakset would contain the identified differentially bound peaks that are insensitive to the choice of between-sample normalization method. Depending on how conservative the researcher wants their differential binding analysis to be, they could amend the proportion of differentially bound peaksets that the peak must belong to for it to belong to the ‘high-confidence’ peakset. For example, a researcher might only require that nine-tenths of the normalization methods’ differentially bound peaksets contain the peak rather than all of them, which would contain at least 185 peaks rather 170 (based on the distinct intersection sizes in Figure 14). Changing the proportion of differentially bound peaksets that the peak must belong to for it to belong to the ‘high-confidence’ peakset could increase the power of their differential binding analysis but might also increase their false discovery rate depending on the underlying structure of the data.

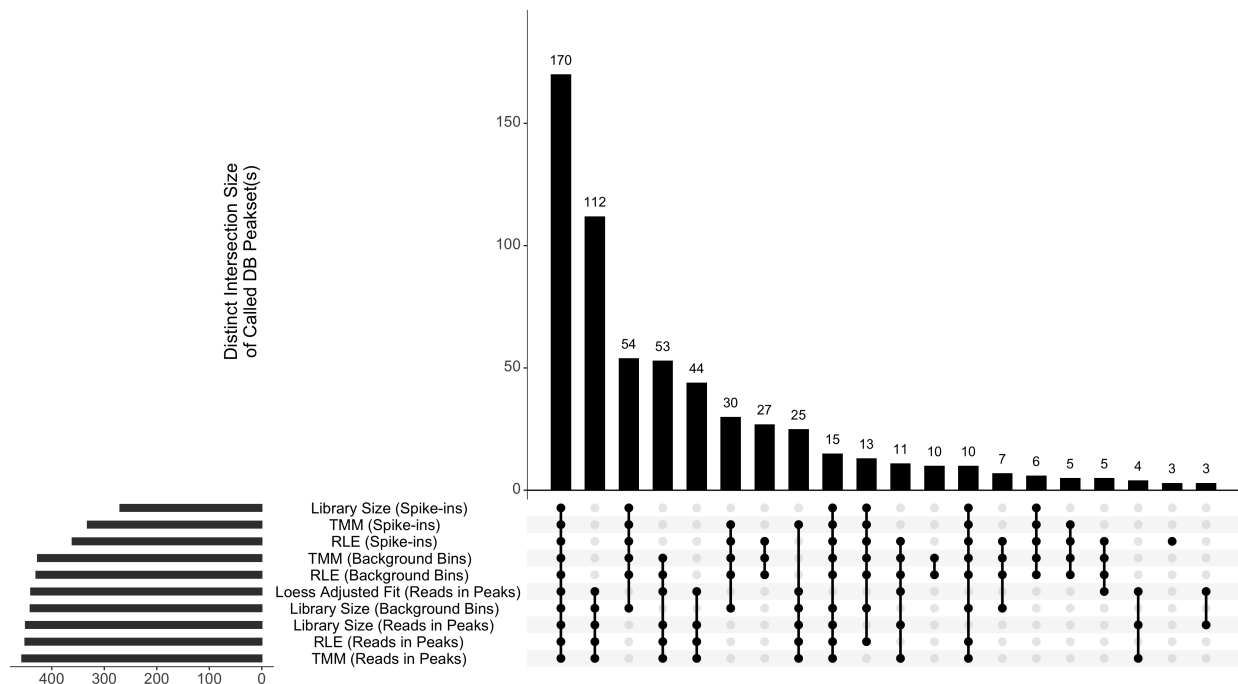


Figure 14: UpSet plot comparing the peaks identified as differentially bound after using each normalization method. The plot visualizes the 20 largest distinct intersection groups between the differentially bound peaksets. The number of peaks identified as differentially bound using each normalization method is given in the horizontal bar plot next to the normalization method’s name. There are 170 peaks that are called as differentially bound in all ten of the normalization methods’ peaksets. These 170 peaks would correspond to the ‘high-confidence’ differentially bound peaks within the experimental study which are insensitive to which between-sample normalization method is used on the data.

## 6 Discussion

Our results show that in running differential binding analyses, the preceding between-sample normalization step is crucial to get right as the technical conditions underlying the selected between-sample normalization method often driving the accuracy of the downstream differential binding analysis (measured by both the average false discovery rate and the power of the test). In some experiments, a researcher will have a sense of whether and how the technical conditions underlying a particular between-sample normalization method are met. For example, if one experimental state causes cell damage or death, the researcher might expect there to be an increase in shearing of chromatin, and with that, a potential increase in the background binding in that specific experimental state. Or, if one experimental state makes it hard to get sufficient numbers of cells to begin the experiment, there could also be an increase in the amount of noise, or background binding, in that particular experimental states. There is also sometimes evidence of global changes in DNA occupancy, such as with a global decrease in H3K27me3 levels [9] or a decrease in CTCF occupancy during the transition from pluripotency to early neuronal lineage commitment for neonatal mouse brains [4].

In cases where the researcher does not have a preconceived notion of any potential technical condition violations, a potential analysis might include implementing multiple between-sample normalization methods on the data, as Ashby *et al.* does, to determine a ‘high-confidence’ differentially bound peakset that is less sensitive to one’s choice of between-sample normalization method [2]. If multiple normalization methods lead to the same set of differentially bound peaks, there is strong evidence toward the differential binding

being the result of genuine differences in the DNA occupancy between experimental states rather than the result of experimental or statistical artifact(s).

## 7 Competing interests

No competing interest is declared.

## 8 Author contributions statement

S.C. conducted the computational study and wrote the manuscript. D.S. ran the biological experiment, provided experimental data, and reviewed the manuscript. J.H. conceived of the study, supported the computational work, and reviewed the manuscript.

## 9 Acknowledgments

S.C. was supported in part by grants from the Pomona College SURP program and Kenneth Cooke Summer Research Fellowship. D.S. was supported in part by NSF CAREER grant 2041395. J.H. was supported in part by NIH GM112625.

## References

- [1] Anders, S. and Huber, W. (2010). Differential expression analysis for sequence count data. *Genome Biology*, 11.
- [2] Ashby, E., Paddock, L., Betts, H. L., Liao, J., Miller, G., Porter, A., Rolloson, L. M., Saada, C., Tang, E., Wade, S. J., Hardin, J., and Schulz, D. (2022). Genomic occupancy of the bromodomain protein bdf3 is dynamic during differentiation of african trypanosomes from bloodstream to procyclic forms. *mSphere*, 7(3):e00023–22.
- [3] Ballman, K. V., Grill, D. E., Oberg, A. L., and Therneau, T. M. (2004). Faster cyclic loess: normalizing rna arrays via linear models. *Bioinformatics*, 20(16):2778–2786.
- [4] Beagan, J., Duong, M., Titus, K., Zhou, L., Cao, Z., Ma, J., Lachanski, C., Gillis, D., and Phillips-Cremins, J. (2017). YY1 and CTCF orchestrate a 3D chromatin looping switch during early neural lineage commitment. *Genome Research*.
- [5] Benjamini, Y. and Hochberg, Y. (1995). Controlling the false discovery rate: A practical and powerful approach to multiple testing. *Journal of the Royal Statistical Society. Series B (Methodological)*, 57(1).
- [6] Blanco, E., Di Croce, L., and Aranda, S. (2021). Spikchip: a novel computational methodology to compare multiple chip-seq using spike-in chromatin. *NAR Genomics and Bioinformatics*, 3.
- [7] Bonhoure, N., Bounova, G., Bernasconi, D., Praz, V., Lammers, F., Canella, D., Willis, I. M., Herr, W., Hernandez, N., Delorenzi, M., and Consortium, C. (2014). Quantifying chip-seq data: a spiking method providing an internal reference for sample-to-sample normalization. *Genome Res.*, 7.
- [8] Chen, Y., Chen, L., Lun, A. T. L., Baldoni, P. L., and Smyth, G. K. (2024). edger 4.0: powerful differential analysis of sequencing data with expanded functionality and improved support for small counts and larger datasets. *bioRxiv*.
- [9] de Sousa, J. A., Wong, C.-W., Dunkel, I., Owens, T., Voigt, P., Hodgson, A., Baker, D., Schulz, E. G., Reik, W., Smith, A., Rostovskaya, M., and von Meyenn, F. (2023). Epigenetic dynamics during capacitation of na<sup>+</sup>-ve human pluripotent stem cells. *Science Advances*, 9(39):eadg1936.



- [10] Dillies, M.-A., Rau, A., Aubert, J., Hennequet-Antier, C., Jeanmougin, M., Servant, N., Keime, C., Marot, G., Castel, D., Estelle, J., Guernec, G., Jagla, B., Jouneau, L., Laloë, D., Gall, C., Schaëffer, B., Le Crom, S., Guedj, M., and Jaffrézic, F. (2012). A comprehensive evaluation of normalization methods for illumina high-throughput RNA sequencing data analysis. *Briefings in bioinformatics*, 14.
- [11] Dudoit, S., Yang, Y., Callow, M., and Speed, T. (2002). Statistical methods for identifying genes with differential expression in replicated cdna microarray. *Stat Sin*, 12.
- [12] Evans, C., Hardin, J., and Stoebel, D. (2016). Selecting between-sample RNA-seq normalization methods from the perspective of their assumptions. *Briefings in Bioinformatics*, 19.
- [13] Kidder, B. L., Hu, G., and Zhao, K. (2011). Chip-seq: technical considerations for obtaining high-quality data. *Nature Immunology*, 12(10):918–922.
- [14] Lee, J.-Y. (2023). The principles and applications of high-throughput sequencing technologies. *Development & Reproduction*, 27.
- [15] Love, M. I., Huber, W., and Anders, S. (2014). Moderated estimation of fold change and dispersion for RNA-seq data with DESeq2. *Genome Biology*, 15.
- [16] Lun, A. and Smyth, G. (2016a). From reads to regions: A Bioconductor workflow to detect differential binding in ChIP-seq data. *F1000Research*, 4.
- [17] Lun, A. T. L. and Smyth, G. K. (2016b). csaw: a Bioconductor package for differential binding analysis of ChIP-seq data using sliding windows. *Nucleic Acids Research*, 44(5):e45.
- [18] Miller, G., Rollosso, L. M., Saada, C., Wade, S. J., and Schulz, D. (2023). Adaptation of CUT&RUN for use in African trypanosomes. *PLOS ONE*, 18:1–7.
- [19] Nakato, R. and Sakata, T. (2020). Methods for chIP-seq analysis: A practical workflow and advanced applications. *Methods*, 187.
- [20] Park, P. (2009). ChIP-seq: advantages and challenges of a maturing technology. *Nature Reviews Genetics*, 10.
- [21] Robinson, M. D. and Oshlack, A. (2010). A scaling normalization method for differential expression analysis of RNA-seq data. *Genome Biology*, 11.
- [22] Skene, P. J. and Henikoff, S. (2017). An efficient targeted nuclease strategy for high-resolution mapping of DNA binding sites. *eLife*, 6:e21856.
- [23] Stark, R. and Brown, G. (2011). DiffBind differential binding analysis of ChIP-Seq peak data. *In R package version*, 100.
- [24] Steinhäuser, S., Kurzawa, N., Eils, R., and Herrmann, C. (2016). A comprehensive comparison of tools for differential ChIP-seq analysis. *Briefings in bioinformatics*, 17.
- [25] Tu, S., Li, M., Haojie, C., Tan, F., Xu, J., Waxman, D., Zhang, Y., and Shao, Z. (2020). MAnorm2 for quantitatively comparing groups of ChIP-seq samples. *Genome Research*, 31.
- [26] Wu, D.-Y., Bittencourt, D., Stallcup, M. R., and Siegmund, K. D. (2015). Identifying differential transcription factor binding in ChIP-seq. *Frontiers in Genetics*, 6.
- [27] Zhang, Y., Liu, T., Meyer, C., Eeckhoutte, J., Johnson, D., Bernstein, B., Nusbaum, C., Myers, R., Brown, M., Li, W., and Liu, S. (2008). Model-based analysis of ChIP-seq (MACS). *Genome biology*, 9.

## 10 Appendix

### 10.1 The Oracle Normalization Method

In our simulation results, an important basis of comparison is the Oracle, which computes the correct sample-wide size factor based on the population-level simulation parameters. Specifically, the Oracle uses the parameter values that calculate the expected value of the negative binomial distribution, which represents the expected amount of DNA binding within a given peak. Let  $p_{ij}$  denote the proportional share of DNA occupancy in peak  $i$  for sample  $j$  before we simulate any differential DNA occupancy between states, and  $(fc)_{ij}$  represent the fold change in DNA occupancy for peak  $i$  in sample  $j$  relative to a sample in the other experimental state. Finally, let  $(\text{library multiplier})_j$  denote the scalar used to increase the variability in DNA binding between samples. Then, the expected value of the negative binomial distribution, which represents the mean amount of DNA binding in the peak, is defined as follows:

$$\mu_{ij} = \frac{p_{ij} \cdot (fc)_{ij}}{(\text{basesum})_j} \cdot (\text{library multiplier})_j \cdot 600,000 \quad (23)$$

where,

$$(\text{basesum})_j = [(fc)_j]^\top \cdot [p_j] \quad (24)$$

and 600,000 is the expected library size for all samples.

Based on how we compute the expected value of the negative binomial distribution, we define the Oracle's size factor for sample  $j$  as follows, where  $m$  is the total number of samples across the two experimental states we simulate:

$$s_j = \frac{(\text{normFactor})_j}{\prod_{h=1}^m (\text{normFactor})_h^{(1/m)}} \quad (25)$$

where,

$$(\text{normFactor})_j = \frac{(\text{library multiplier})_j}{(\text{basesum})_j} \quad (26)$$

As a result, we obtain the following when we divide the mean read count for peak  $i$  under sample  $j$  (i.e.,  $\mu_{ij}$ ) by the normalization factor for sample  $j$ :

$$\frac{\mu_{ij}}{(\text{normFactor})_j} = p_{ij} \cdot (fc)_{ij} \cdot 600,000 \quad (27)$$

Since  $p_{ij}$  (i.e., the base proportion of DNA occupancy in peak  $i$  in sample  $j$ ) and the expected library size of 600,000 are constant across all the samples in our simulation, only  $(fc)_{ij}$  changes between experimental states. Therefore, when we compare read counts that are normalized by the Oracle across experimental states, we correctly estimate the fold change in DNA occupancy across the experimental states. The geometric mean of normalization factors in the denominator of Equation (25) serves as the pseudo-reference sample for the normalization. In the next section, we provide a toy example to walk through the Oracle and the population-level simulation parameters it utilizes to compute the sample-wide size factor for each replicate.

#### 10.1.1 Oracle Toy Example

Suppose there are two experimental states (A and B) and three peaks within each experimental state (denoted as Peaks 1,2, and 3). The library multipliers for State A and State B are 0.9 and 0.8, respectively. We can find the Oracle normalization factors associated with States A and B in our toy example in Figure 15 by using Equation (26) and leveraging the fact that the library multipliers for State A and State B are 0.9 and 0.8, respectively. Namely, the normalization factors associated with A and B are the following:

$$(\text{normFactor})_A = \frac{0.9}{1} = 0.9 \quad (28)$$

$$(\text{normFactor})_B = \frac{0.8}{\frac{4}{3}} = 0.6 \quad (29)$$

Then, we can find the Oracle size factor for each experimental state by using Equation (25).

$$s_A = \frac{0.9}{\sqrt{0.6 \cdot 0.9}} = 1.2247 \quad (30)$$

$$s_B = \frac{0.6}{\sqrt{0.6 \cdot 0.9}} = 0.8165 \quad (31)$$

Dividing the raw read counts for States A and B given in Figure 15(d) by their respective Oracle size factors of 1.04447 and 0.95743 gives us the Oracle normalized read counts given in Figure 15(e). Table 2 shows the calculations for the Oracle-normalized read counts.

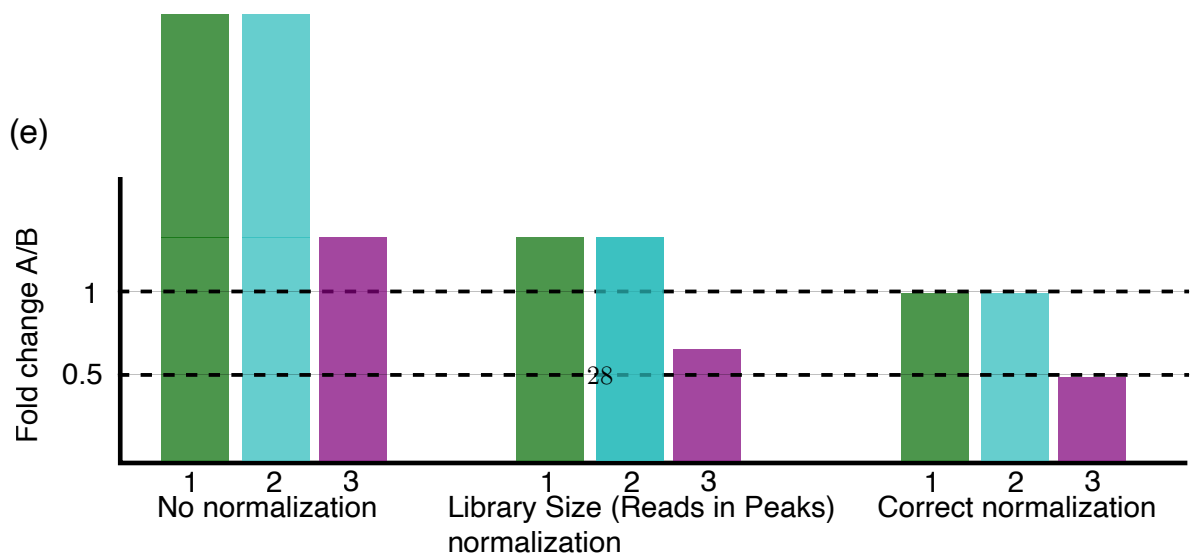
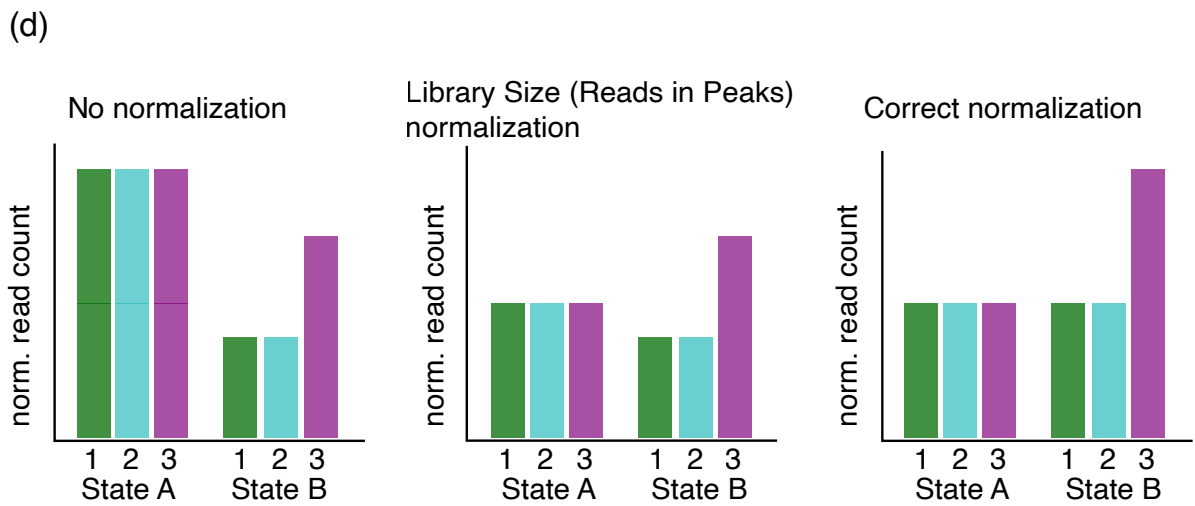
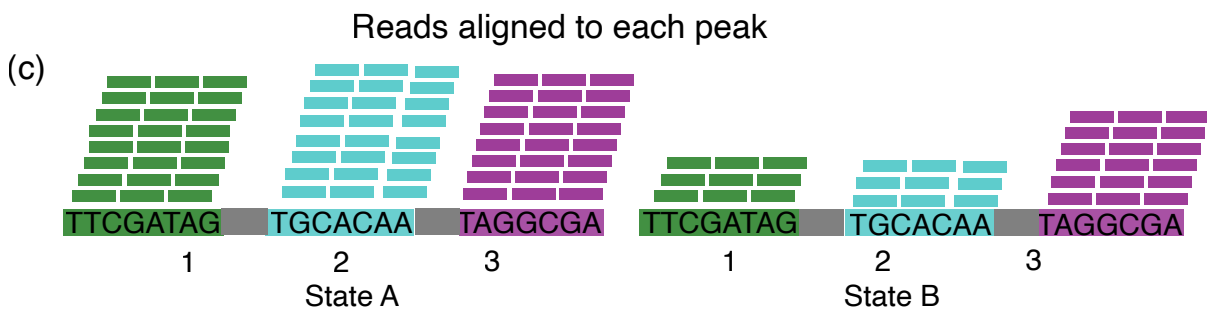
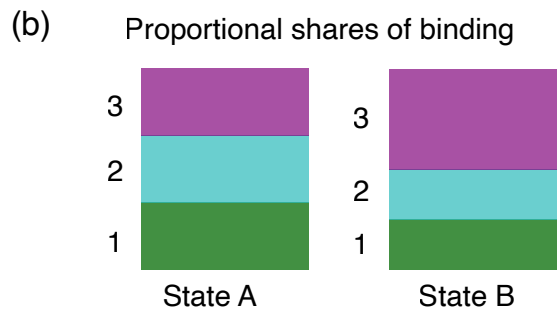
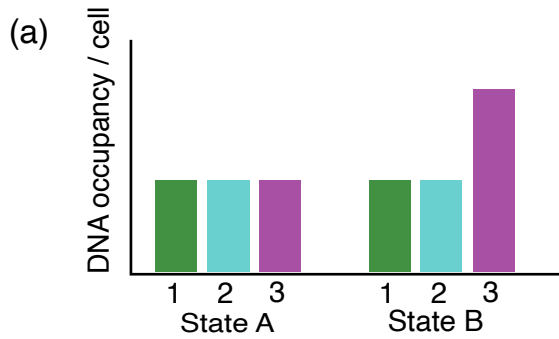
From the Oracle-normalized read counts computed in Table 2, we would conclude that Peaks 1 and 2 are *not* differentially bound and that Peak 3 *is* differentially bound, with two times more DNA binding in State B than State A. As shown in Plots (e) and (f) of Figure 15, the Oracle-normalized DNA binding results correctly align with the amount of DNA occupancy (per cell) depicted in Plot (a) of Figure 15. Thus, the toy example demonstrates that the Oracle normalization method correctly normalizes between samples by leveraging the population-wide simulation parameters.

Table 2: Oracle Normalized Read Counts. The columns correspond to the experimental state associated with the raw read count, and the rows correspond to the peak associated with the raw read count. Each entry is the Oracle normalized read count for the specific peak, which is found by multiplying the raw read count depicted in Plot (d) of Figure 15 by the size factors calculated in Equations (30) and (31).

	Norm. read count (A)	Norm. read count (B)
Peak 1	54/1.2247 = 44.0906	36/0.8165 = 44.0906
Peak 2	54/1.2247 = 44.0906	36/0.8165 = 44.0906
Peak 3	54/1.2247 = 44.0906	72/0.8165 = 88.1812

## 10.2 Simulation Results: 10 Replicates per Experimental State

In what follows, we provide figures which are similar to those in the main manuscript but include 10 samples per experimental state (as opposed to 4 samples per experimental state in the main simulation results section). The patterns seen above with 4 samples are equivalent to those observed here with 10 samples.



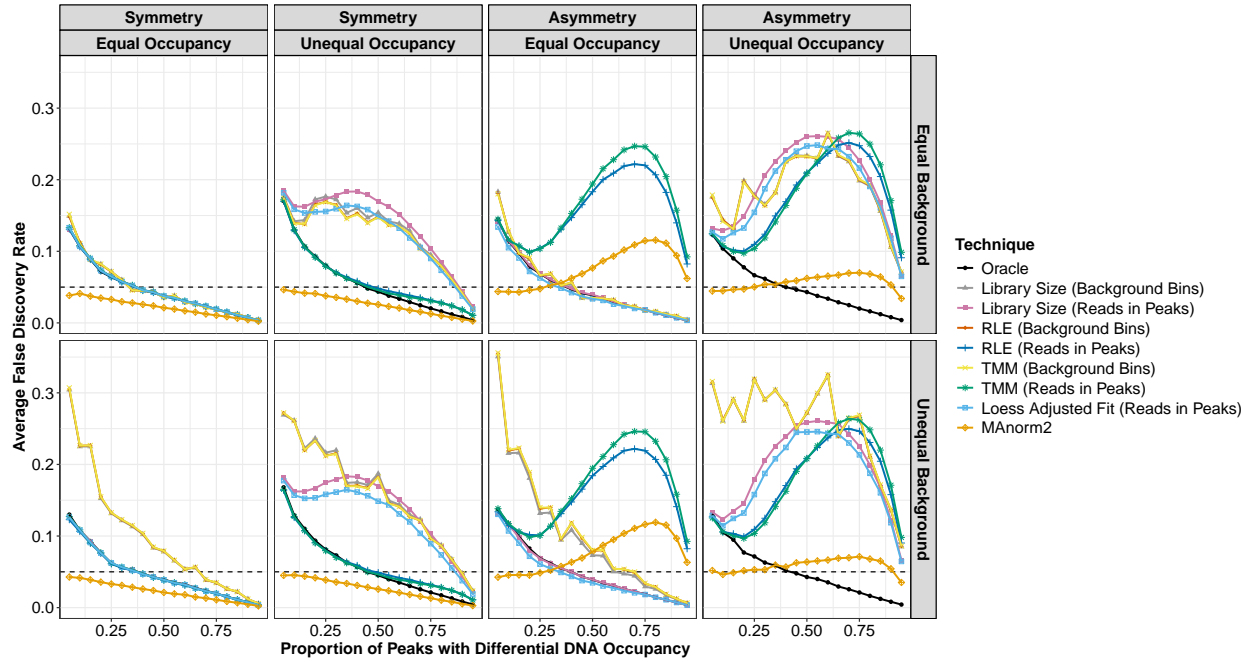


Figure 7: The average false discovery rate for each normalization method, faceted by simulation condition (4 replicates per experimental state and 100 simulation iterations per combination of simulation condition and proportion of peaks with differential DNA occupancy). The horizontal axis is the proportion of peaks with differential DNA occupancy, and the vertical axis is the average false discovery rate. When a curve is below the dashed horizontal black line, then the associated normalization method (on average) successfully controls the false discovery rate at a level of 0.05 for the given proportion of peaks with differential DNA occupancy. We consider normalization methods that track with the Oracle (the solid black line) to be performing well with respect to the average false discovery rate in our simulation.

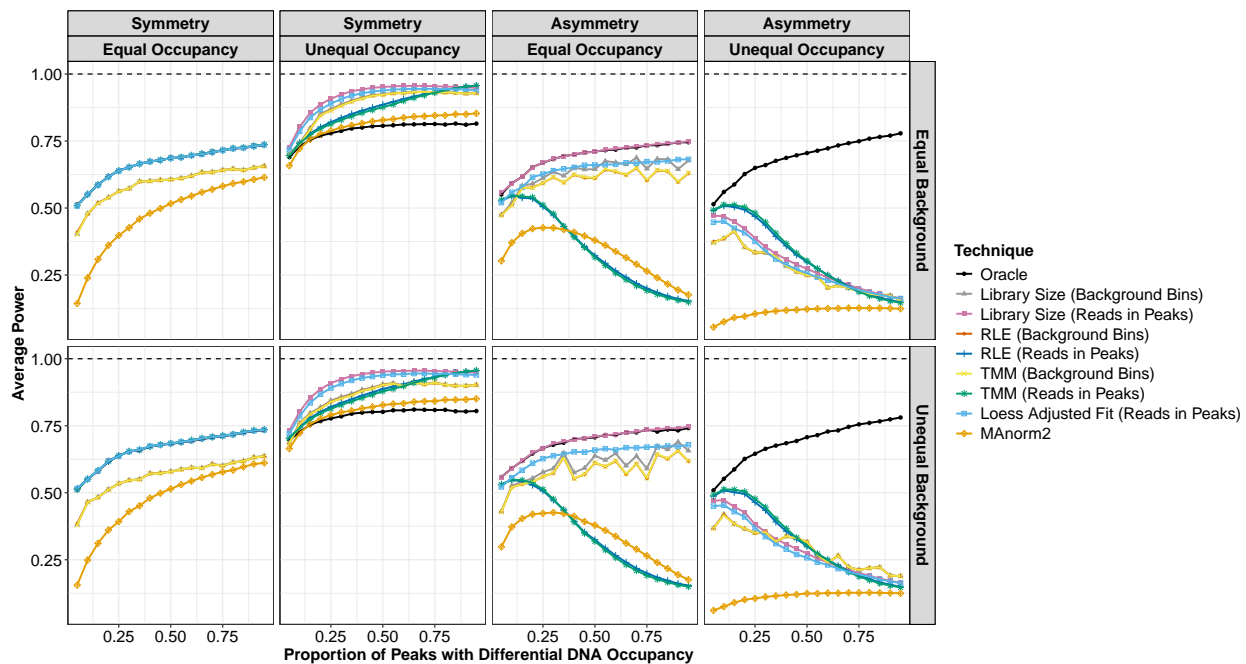


Figure 8: The average power for each normalization method, faceted by simulation condition (4 replicates per experimental state and 100 simulation iterations per combination of simulation condition and proportion of peaks with differential DNA occupancy). The horizontal axis is the proportion of peaks with differential DNA occupancy, and the vertical axis is the average power. The nearer a curve is to the dashed horizontal black line at 1, the higher power the associated normalization method has (on average) for the given proportion of peaks with differential DNA occupancy.

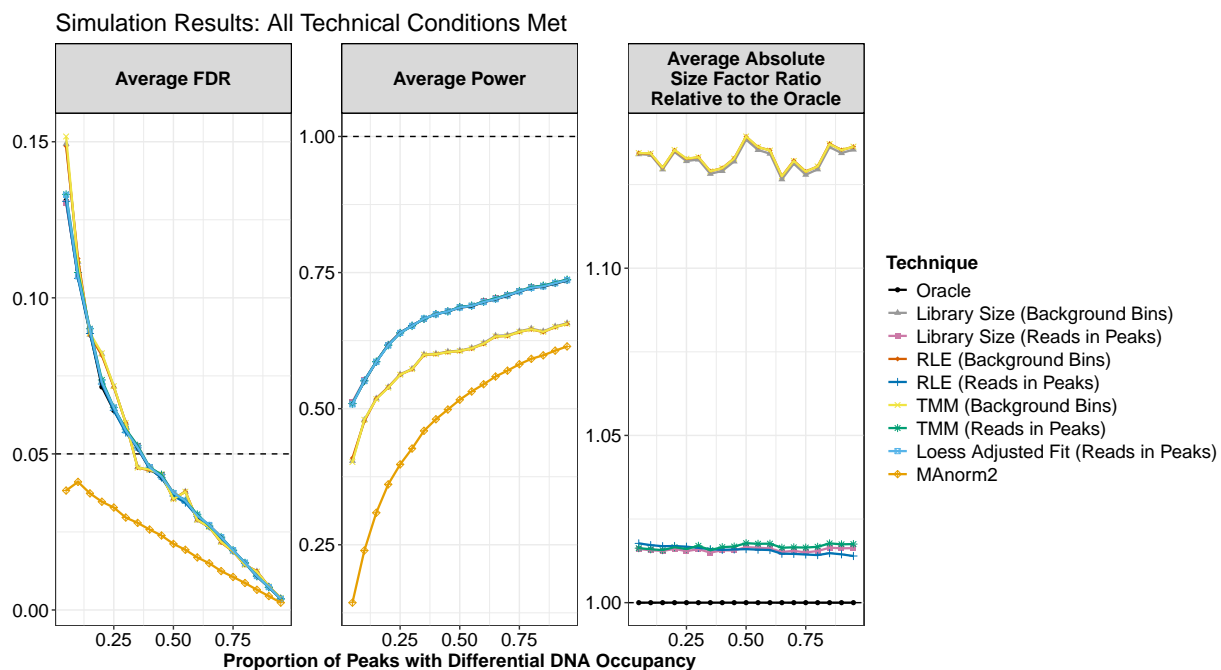


Figure 9: Simulation results when all three technical conditions are met, with four replicates per experimental state. The horizontal axis is the proportion of peaks with differential DNA occupancy, and the vertical axis is the value for each simulation metric. The figure is faceted such that each subplot represents one of the three simulation metrics (note the scale change between each facet in the figure). The leftmost plot is the average false discovery rate, where the horizontal black line represents the 0.05 FDR threshold we set. The middle plot is the average power, where the horizontal black line at 1 represents the highest possible average power. The rightmost plot is the average absolute size factor ratio relative to the Oracle, where the horizontal line at 1 represents the Oracle’s average absolute size factor ratio with itself. Thus, a normalization method is taken to track closely with the Oracle if its curve is close to the horizontal black line at 1 in the rightmost plot. Recall that MAnorm2 and Loess Adjusted Fit (Reads in Peaks) do not generate sample-wide size factors and so do not have curves in the rightmost plot of the figure.

Simulation Results: Unequal Total DNA Occupancy

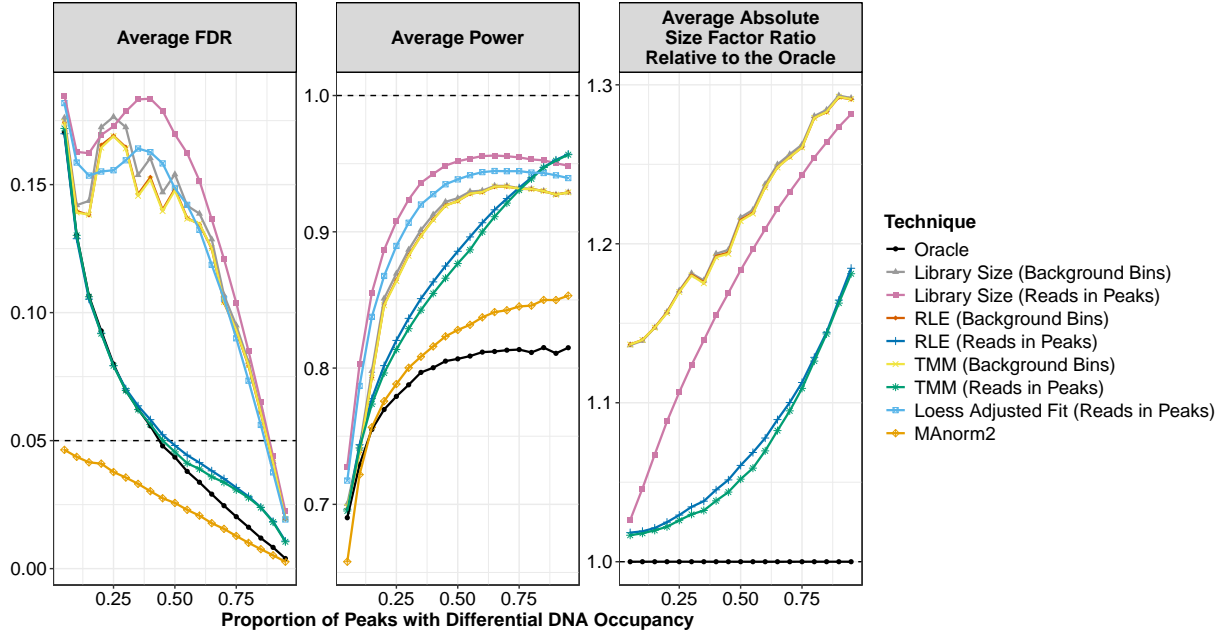


Figure 11: Simulation results when only equal total DNA occupancy between experimental states is violated, with four replicates per experimental state. The horizontal axis is the proportion of peaks with differential DNA occupancy, and the vertical axis is the value for each simulation metric. The figure is faceted such that each subplot represents one of the three simulation metrics (note the scale change between each facet in the figure). The leftmost plot is the average false discovery rate, where the horizontal black line represents the 0.05 FDR threshold we set. The middle plot is the average power, where the horizontal black line at 1 represents the highest possible average power. The rightmost plot is the average absolute size factor ratio relative to the Oracle, where the horizontal line at 1 represents the Oracle’s average absolute size factor ratio with itself. Thus, a normalization method is taken to track closely with the Oracle if its curve is close to the horizontal black line at 1 in the rightmost plot. Recall that MAnorm2 and Loess Adjusted Fit (Reads in Peaks) do not generate sample-wide size factors and so do not have curves in the rightmost plot of the figure.



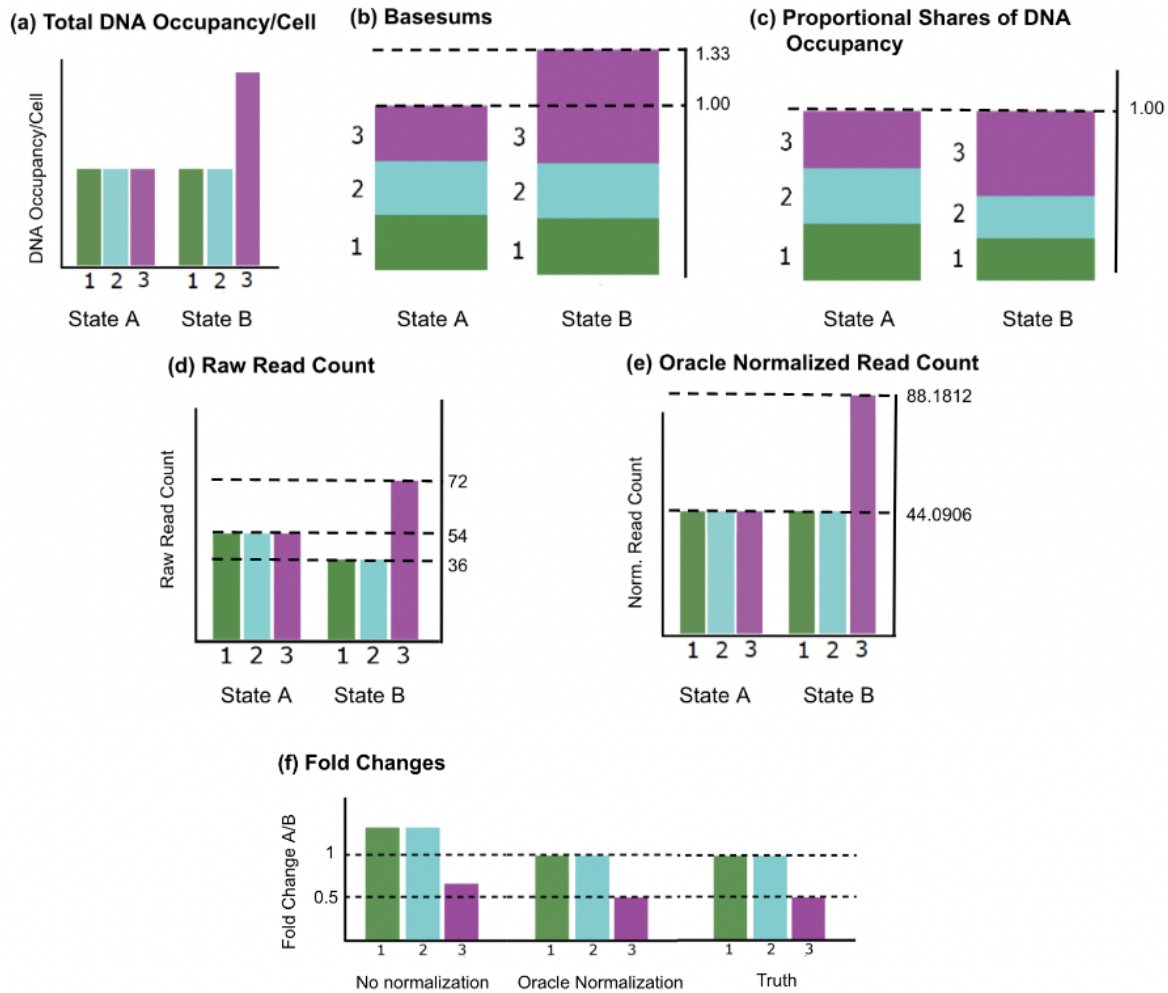


Figure 15: Illustration of Oracle Normalization Method. Plot (a) represents the DNA occupancy (per cell) for each peak in States A and B. Plot (b) is the corresponding basesums for States A and B. Plot (c) provides the proportional shares of DNA occupancy for the peaks for States A and B. The raw read counts are generated through the general process outlined in Equation (23) and are depicted in Plot (d). Using the raw read counts, Peaks 1 and 2 appear differentially bound even though they do not have different DNA occupancy in Plot (f). Additionally, even though Peak 3 has 1/2 as much DNA occupancy in State A as compared to B in Plot (a), it appears to have 2/3 as much in Plot (f). Note that when we normalize our toy data using the Oracle, the fold changes associated with the Oracle normalized read counts in Plot (e) match the *true* fold changes in the DNA occupancy between the states depicted in Plot (f).

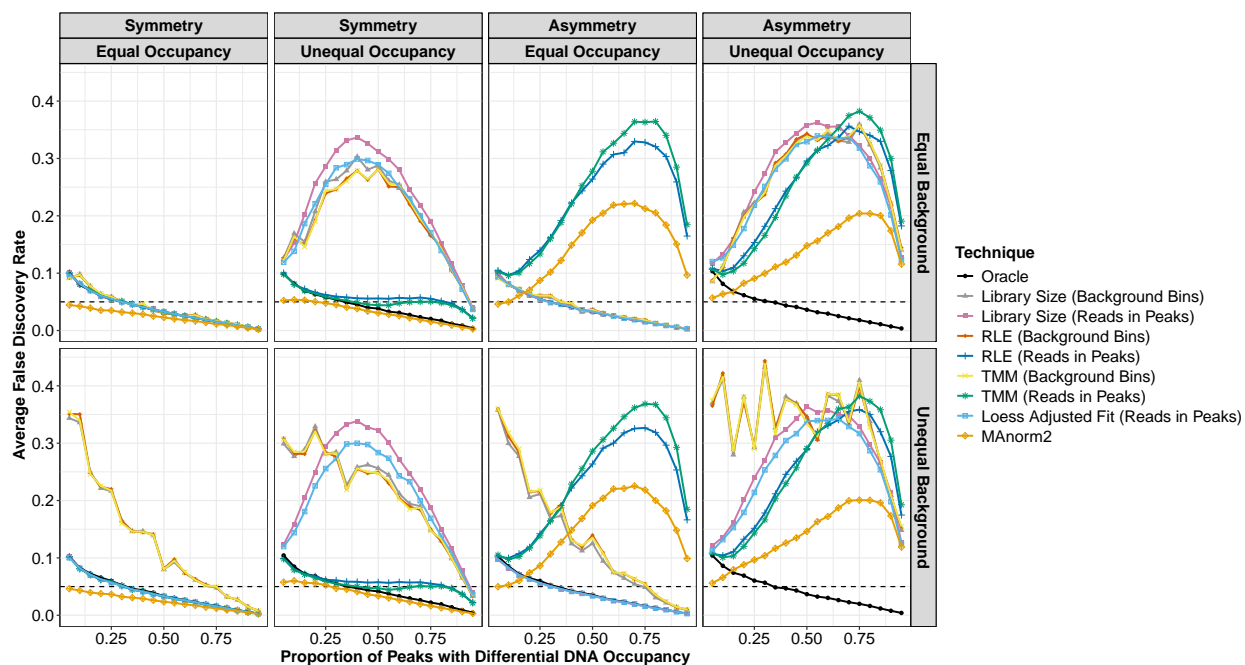


Figure 16: Similar to Figure 7, except now with 10 samples in each experimental state. The average false discovery rate for each normalization method, faceted by simulation condition (10 replicates per experimental state and 50 simulation iterations per combination of simulation condition and proportion of peaks with differential DNA occupancy). The horizontal axis is the proportion of peaks with differential DNA occupancy, and the vertical axis is the average false discovery rate. When a curve is below the dashed horizontal black line, then the associated normalization method (on average) successfully controls the false discovery rate at a level of 0.05 for the given proportion of peaks with differential DNA occupancy. We consider normalization methods that track with the Oracle (the solid black line) to be performing well with respect to the average false discovery rate in our simulation.

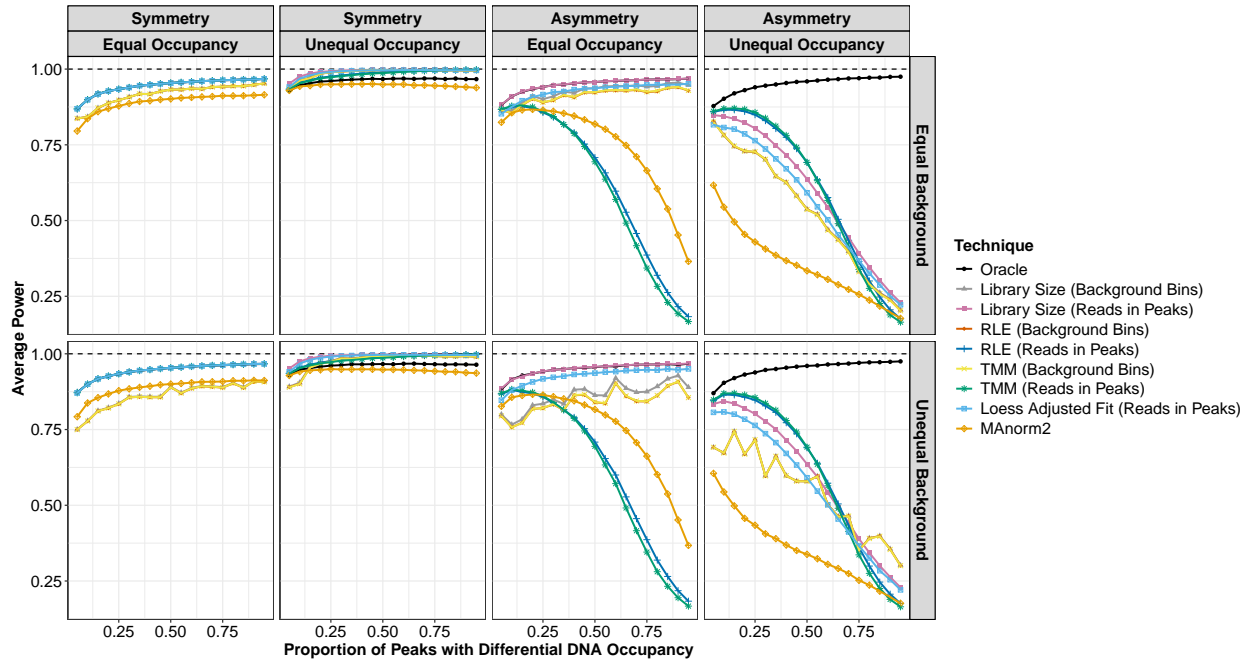


Figure 17: Similar to Figure 8, except now with 10 samples in each experimental state. The average power for each normalization method, faceted by simulation condition (10 replicates per experimental state and 50 simulation iterations per combination of simulation condition and proportion of peaks with differential DNA occupancy). The horizontal axis is the proportion of peaks with differential DNA occupancy, and the vertical axis is the average power. The nearer a curve is to the dashed horizontal black line at 1, the higher power the associated normalization method has (on average) for the given proportion of peaks with differential DNA occupancy.

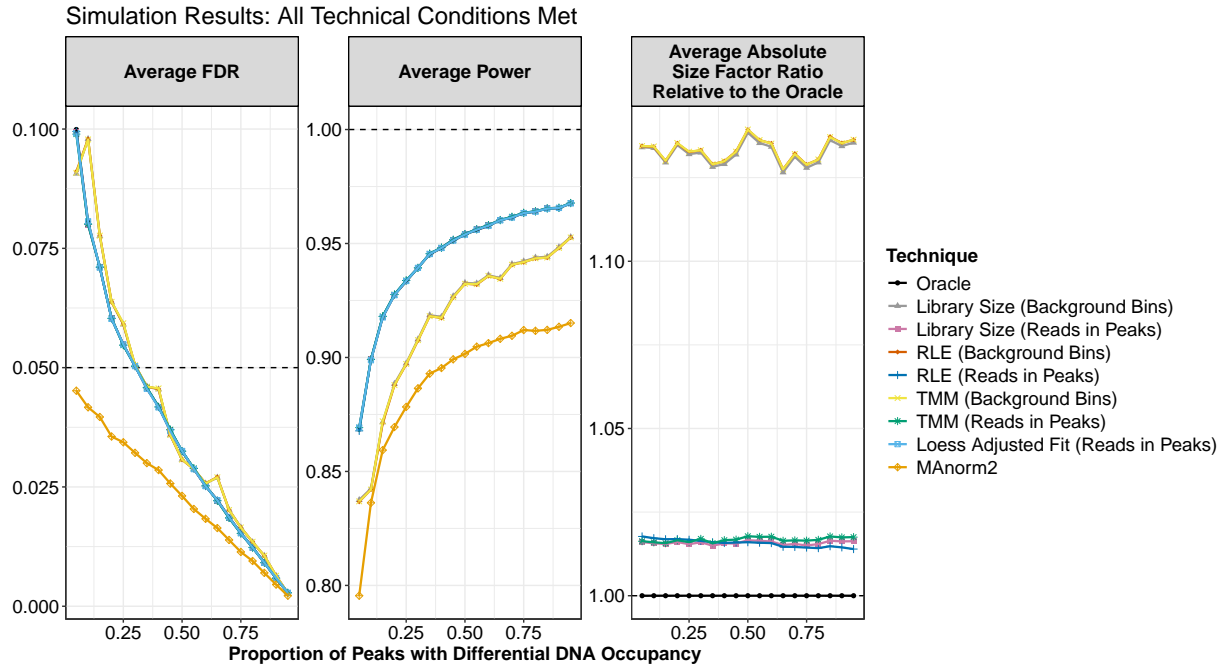


Figure 18: Similar to Figure 9, except now with 10 samples in each experimental state. Simulation results when all three technical conditions are met, with four replicates per experimental state. The horizontal axis is the proportion of peaks with differential DNA occupancy, and the vertical axis is the value for each simulation metric. The figure is faceted such that each subplot represents one of the three simulation metrics (note the scale change between each facet in the figure). The leftmost plot is the average false discovery rate, where the horizontal black line represents the 0.05 FDR threshold we set. The middle plot is the average power, where the horizontal black line at 1 represents the highest possible average power. The rightmost plot is the average absolute size factor ratio relative to the Oracle, where the horizontal line at 1 represents the Oracle's average absolute size factor ratio with itself. Thus, a normalization method is taken to track closely with the Oracle if its curve is close to the horizontal black line at 1 in the rightmost plot. Recall that MAnorm2 and Loess Adjusted Fit (Reads in Peaks) do not generate sample-wide size factors and so do not have curves in the rightmost plot of the figure.

Simulation Results: Asymmetric Differential DNA Occupancy

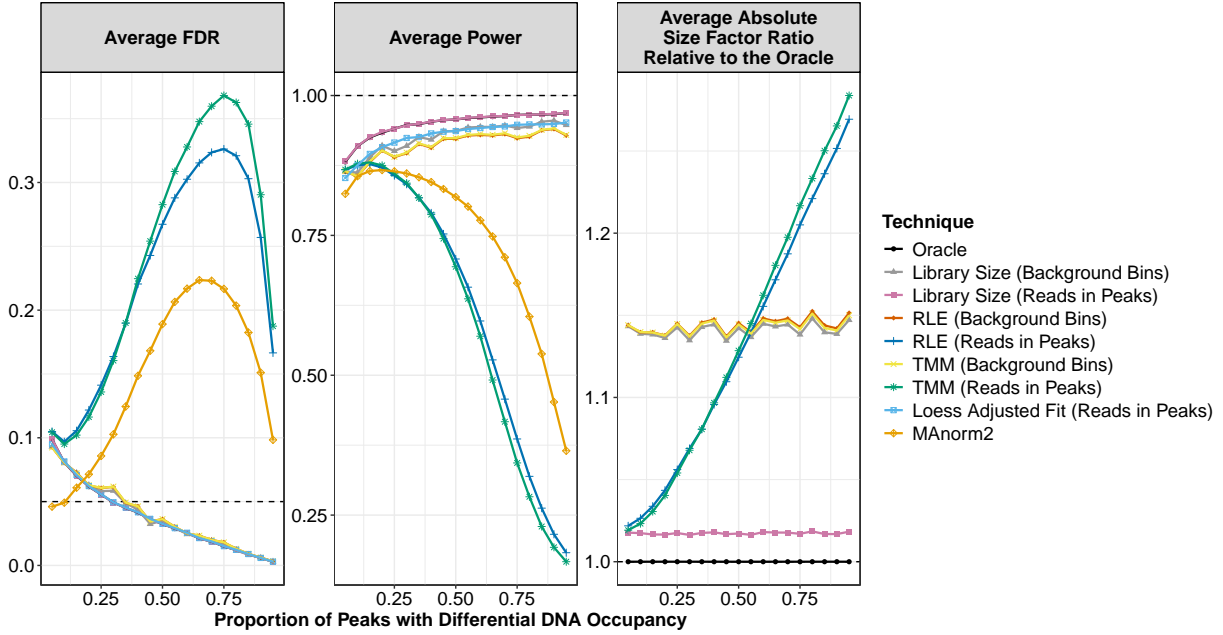


Figure 19: Similar to Figure 10, except now with 10 samples in each experimental state. Simulation results when only symmetric differential is violated, with four replicates per experimental state. The horizontal axis is the proportion of peaks with differential DNA occupancy, and the vertical axis is the value for each simulation metric. The figure is faceted such that each subplot represents one of the three simulation metrics (note the scale change between each facet in the figure). The leftmost plot is the average false discovery rate, where the horizontal black line represents the 0.05 FDR threshold we set. The middle plot is the average power, where the horizontal black line at 1 represents the highest possible average power. The rightmost plot is the average absolute size factor ratio relative to the Oracle, where the horizontal line at 1 represents the Oracle’s average absolute size factor ratio with itself. Thus, a normalization method is taken to track closely with the Oracle if its curve is close to the horizontal black line at 1 in the rightmost plot. Recall that MAnorm2 and Loess Adjusted Fit (Reads in Peaks) do not generate sample-wide size factors, and so do not have curves in the rightmost plot of the figure.

Simulation Results: Unequal Total DNA Occupancy

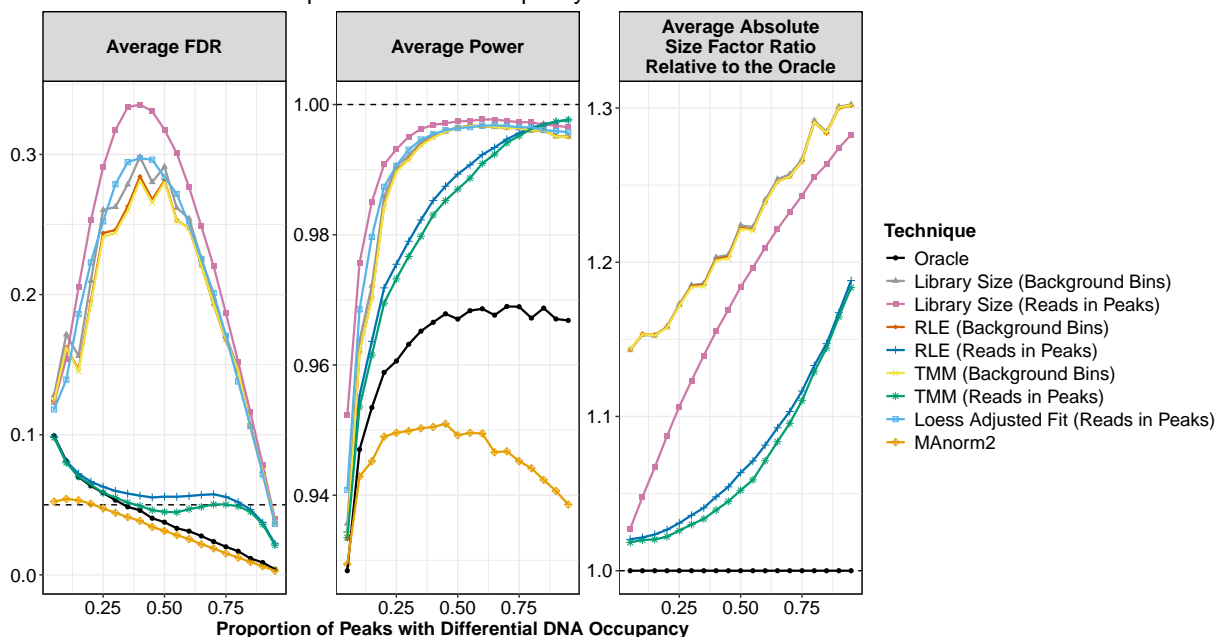


Figure 20: Similar to Figure 11, except now with 10 samples in each experimental state. Simulation results when only equal total DNA occupancy between experimental states is violated, with four replicates per experimental state. The horizontal axis is the proportion of peaks with differential DNA occupancy, and the vertical axis is the value for each simulation metric. The figure is faceted such that each subplot represents one of the three simulation metrics (note the scale change between each facet in the figure). The leftmost plot is the average false discovery rate, where the horizontal black line represents the 0.05 FDR threshold we set. The middle plot is the average power, where the horizontal black line at 1 represents the highest possible average power. The rightmost plot is the average absolute size factor ratio relative to the Oracle, where the horizontal line at 1 represents the Oracle's average absolute size factor ratio with itself. Thus, a normalization method is taken to track closely with the Oracle if its curve is close to the horizontal black line at 1 in the rightmost plot. Recall that MAnorm2 and Loess Adjusted Fit (Reads in Peaks) do not generate sample-wide size factors and so do not have curves in the rightmost plot of the figure.

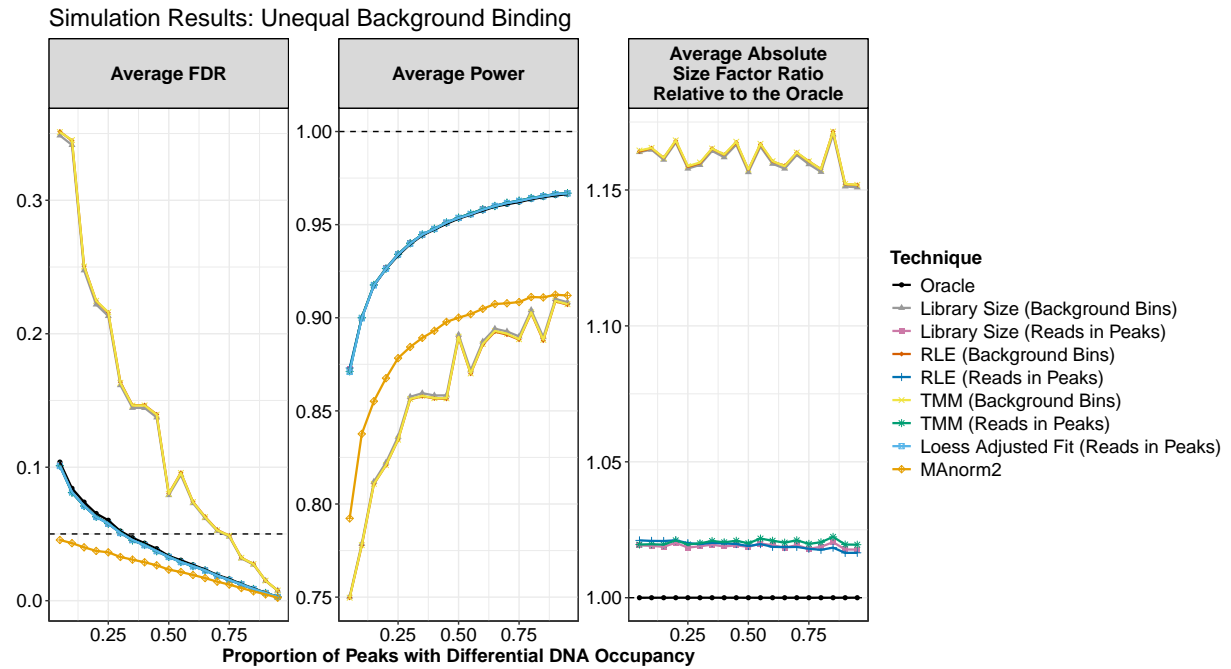


Figure 21: Similar to Figure 12, except now with 10 samples in each experimental state. Simulation results when only equal background binding between experimental states is violated, with four replicates per experimental state. The horizontal axis is the proportion of peaks with differential DNA occupancy, and the vertical axis is the value for each simulation metric. The figure is faceted such that each subplot represents one of the three simulation metrics (note the scale change between each facet in the figure). The leftmost plot is the average false discovery rate, where the horizontal black line represents the 0.05 FDR threshold we set. The middle plot is the average power, where the horizontal black line at 1 represents the highest possible average power. The rightmost plot is the average absolute size factor ratio relative to the Oracle, where the horizontal line at 1 represents the Oracle's average absolute size factor ratio with itself. Thus, a normalization method is taken to track closely with the Oracle if its curve is close to the horizontal black line at 1 in the rightmost plot. Recall that MAnorm2 and Loess Adjusted Fit (Reads in Peaks) do not generate sample-wide size factors and so do not have curves in the rightmost plot of the figure.